APPLICATIONS OF RAMAN SPECTROSCOPY

Jeanette G. GRASSELLI and Marcia K. SNAVELY

The Standard Oil Company, Research and Development Division, Cleveland, Ohio 44128, U.S.A.

and

Bernard J. BULKIN

Chemistry Department, Polytechnic Institute of New York, Brooklyn, New York 11201, U.S.A.

NORTH-HOLLAND PUBLISHING COMPANY - AMSTERDAM

PHYSICS REPORTS (Review Section of Physics Letters) 65, No. 4 (1980) 231–344. North-Holland Publishing Company

APPLICATIONS OF RAMAN SPECTROSCOPY

Jeanette G. Grasselli and Marcia K. Snavely

The Standard Oil Company, Research and Development Division, Cleveland, Ohio 44128, U.S.A.

and

Bernard J. BULKIN

Chemistry Department, Polytechnic Institute of New York, Brooklyn, New York 11201, U.S.A.

Received February 1980

Contents:

1. Introduction 233
2. Theory of Raman spectroscopy 235
3. Development of modern Raman instrumentation 237
4. Techniques 239
   4.1. Sample handling 239
   4.2. Micro work 240
   4.3. The Raman microprobe 240
   4.4. The rotating cell 242
   4.5. Quantitative analysis 244
   4.6. Separated fractions 246
   4.7. Resonance Raman 250
5. Group frequencies 251
   5.1. Carbon halogen stretching 255
   5.2. Triple bond stretching, C≡C and C≡N 257
   5.3. Aromatic structures 257
   5.4. Other characteristic vibrations 258
6. Raman applications to organic chemistry 258
   6.1. Structure elucidation 258
   6.2. Studies of structurally related compounds 260
   6.3. Conformation studies and molecular symmetry 261
   6.4. Molecular potential functions 262
   6.5. Physical properties 262
7. Raman applications to polymers 263
   7.1. Polarization measurements of polymers 266
   7.2. Morphological effects 269
   7.3. Other polymer features 269
   7.4. Detection of impurities in polymer films 270
   7.5. Miscellaneous polymer applications 271
   7.6. Future of Raman polymer studies 272
8. Raman applications to biological systems 272
   8.1. Peptides and proteins 273
   8.2. Nucleotides and nucleic acids 276
   8.3. Resonance Raman spectra of biological systems 280
   8.4. Lipids and membranes 285
9. Liquid crystals 288
10. Raman applications to inorganic and organometallic chemistry 297
   10.1. Structural studies: molecular species 297
   10.2. Structural studies: colored ionic species 298
   10.3. Structural studies: colored coordination compounds 299
   10.4. Structural studies: glasses and quartz 299
   10.5. Structural studies: carbon compounds 300
   10.6. Structural studies: sulfur compounds 300
   10.7. Structural studies involving changes of state and phase transitions 301
   10.8. Molten state 302
   10.9. Equilibrium, dissociation and redistribution reactions 302
   10.10. Complex ions 303
   10.11. Resonance Raman of inorganic molecules 303
   10.12. Minerals 304
11. Adsorbed species and surfaces 305

Single orders for this issue

PHYSICS REPORTS (Review Section of Physics Letters) 65, No. 4 (1980) 231–344.

Copies of this issue may be obtained at the price given below. All orders should be sent directly to the Publisher. Orders must be accompanied by check.

Single issue price Dfl. 48.00, postage included.

12. Catalyst research 308
12.1. Techniques 308
12.2. Heated cell 309
12.3. Surface vs. bulk structures 310
13. Raman applications to the petroleum industry 311
14. Miscellaneous Raman applications 316
14.1. Barbiturates 316
14.2. Coals 318
14.3. Water pollution 319
14.4. Air pollution 321
14.5. Flames and combustion 321
15. Raman band shapes as a source of information 323
16. Non-linear effects, particularly CARS 328
17. Recent developments in instrumentation 333
17.1. Image intensifiers and vidicons 333
17.2. Rapid scanning Raman spectroscopy 335
18. In conclusion: Where have we come from and where are we going? 335
References 336

1. Introduction

Infrared spectroscopy has been widely recognized for years as an important, powerful and elegant tool for the analysis and identification of materials and for the study of structures and dynamics of molecules. Raman spectroscopy, though theoretically richer in vibrational information about molecules and possessing some fundamental practical advantages over infrared spectroscopy, lagged behind IR in development as an analytical tool due to experimental and instrumental problems in obtaining spectra. With the advent of the laser as a source in the early 1960's, commercial Raman instruments rapidly developed. Other instrumentation advances also contributed to a renaissance in this technique's utility.

To better appreciate the reasons for this intense renewed interest in Raman, it is instructive to compare some of the advantages and disadvantages of Raman and IR with respect to instrumentation, sampling handling, and applications. Tables 1–3 taken from a comparison by Sloane [1] summarize such information. Since Raman scattering occurs in the visible spectrum, the optics of the instrument are simple. Sensitive detectors with high signal-to-noise ratios are available. The intrinsic weakness of the Raman effect (Raman lines are about 10^{-6} the intensity of the exciting line) necessitates the use of an intense monochromatic light source, and, as such, the laser is ideal. A decided advantage of Raman

Table 1
Sampling handling

	Raman	IR
A. General applicability	95%	99%
B. Sample limitations	Color; fluorescence	Single crystals: metals; aqueous solutions
C. Ease of sample preparation	Very simple	Variable
1. Liquids	Very simple	Very simple
2. Powders	Very simple	More difficult
3. Single crystals	Very simple	Very difficult
4. Polymers	Very simple (but see B)	More difficult
5. Single fibers	Possible	Difficult
6. Gases and vapors	Now possible	Simple
D. Cells	Very simple (glass)	More complex (akali halide)
E. Micro work	Good (<1 μg)	Good (<1 μg)
F. Trace work	Sometimes	Sometimes
G. High and low temperature	Moderately simple	Moderately simple

Table 2
Instrumentation

	Raman	IR
A. Relative complexity	Moderate	Slightly greater
B. Source	Laser	Blackbody
C. Detector	Photomultiplier tube	Thermal
D. Resolution	ca. 0.25 cm^{-1}	ca. 0.20 cm^{-1}
E. Principal limitation	Energy	Energy
F. Wavenumber range	10–4000 Δ cm^{-1}	180–4000 cm^{-1} (one instrument) 10–400 cm^{-1} (second instrument)
G. Purge requirement	No	Yes
H. Photometry	Emission single beam	Absorption double beam

is that the entire spectrum is obtained with the same instrument and cell, giving more information in a shorter time.

Infrared is applicable to almost any kind of sample but some materials (intractable polymers, single crystals, and aqueous solutions) are quite difficult to handle. In Raman spectroscopy, sample preparation is remarkably simple and the capability for using glass or quartz cells is a marked advantage. Its principal limitation is with highly colored or fluorescing materials.

Both Raman and infrared spectra are necessary to completely describe the vibrational motions of molecules. They are highly complementary. Although some vibrational modes may be common to both the IR and Raman, these two forms of spectroscopy arise from different physical processes governed by specific selection rules, and the information content in the two techniques is a function of the molecular symmetry and polarity. Symmetric vibrations and nonpolar groups are most easily studied by Raman, antisymmetric vibrations and polar groups by infrared. At the empirical level, both techniques are excellent "fingerprints" for qualitative identification of molecules for the analytical chemist. Infrared spectroscopy holds an advantage in the huge number of reference spectra which are available, but group frequencies are equally well-recognized and useful in both methods. Without question, the possibility of examining aqueous solutions in the Raman gives it a tremendous advantage over infrared in biological and inorganic chemistry and is of immense importance.

In this review, we highlight a few aspects of modern Raman spectroscopy and its application to chemical problems. It would be impossible to be comprehensive. Instead, we have provided a brief introduction to Raman spectroscopy regarding instrumentation, techniques, and group frequencies and

Table 3
Applications

	Raman	IR
A. Fingerprinting	Excellent	Excellent
B. Best vibrations	Symmetric	Asymmetric
C. Assignment work	Excellent	Very good
D. Group frequencies	Excellent	Excellent
E. Aqueous solutions	Very good	Very difficult
F. Quantitative analysis	More difficult	Good
G. Low frequency modes	Excellent	Difficult

then selected a number of areas and examples of interest, in the hopes of giving a flavor of the type of work now being done. The depth of treatment of particular areas is, to some extent, more a reflection of our own interests and expertise than of the regard in which we hold the work of our colleagues.

2. Theory of Raman spectroscopy

For an introduction to all aspects of the theory of Raman spectroscopy, a recent book by Long [2] is excellent; but a brief review here of the theory is helpful for putting Raman spectroscopy in perspective with relation to infrared spectroscopy and to help illustrate its importance. In infrared spectroscopy, it is the vibrational energy levels of the molecule which are involved. Molecules can scatter visible light and the scattering may be elastic or inelastic in nature. Inelastic scattering is the basis of the Raman effect, and it results in a gain or loss of energy by the photon after its collision with the molecule. This is illustrated in the energy level diagram in fig. 1. The first vibrational energy level of a diatomic molecule is designated ν_1 and absorption of photons with energy equal to $h\nu_1$ would give rise to the infrared spectrum. If monochromatic radiation of frequency ν_0 falls on a molecule, it is excited to a virtual state. (The virtual state must be lower than the electronic energy of the molecule so that no absorption of the beam occurs.) The molecule can return directly to the ground state, emitting light of energy $h\nu_0$ (Rayleigh line) or it can return to the first vibrational energy level, emitting a photon whose energy has been decreased by $h(\nu_0 - \nu_1)$. Molecules which are already in a vibrational excited level can also scatter light elastically and emit photons of unchanged energy (Rayleigh line), or they can return to the ground state by emitting a photon whose energy has been increased by $h(\nu_0 + \nu_1)$. These shifted lines constitute the Raman spectrum, and those which appear at lower frequency are called Stokes lines; those shifted to higher frequency are called anti-Stokes lines. Since the number of molecules which exist in the excited state is governed by the Boltzmann distribution, the Stokes lines are much more intense than the anti-Stokes lines. This is illustrated in the Raman spectrum of CCl_4 shown in fig. 2. The shifts in frequency of the scattered photons in the Raman effect correspond to the vibrational energy levels of the molecule as observed in infrared spectroscopy. It should be noted that it is also possible to observe rotational and electronic Raman spectra, but at present the most useful information is derived from the study of changes in the vibrational energy of molecules.

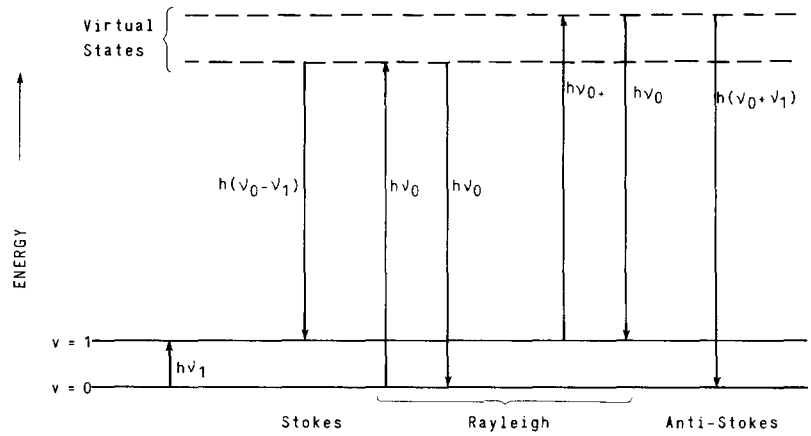

Fig. 1. Energy level diagram.

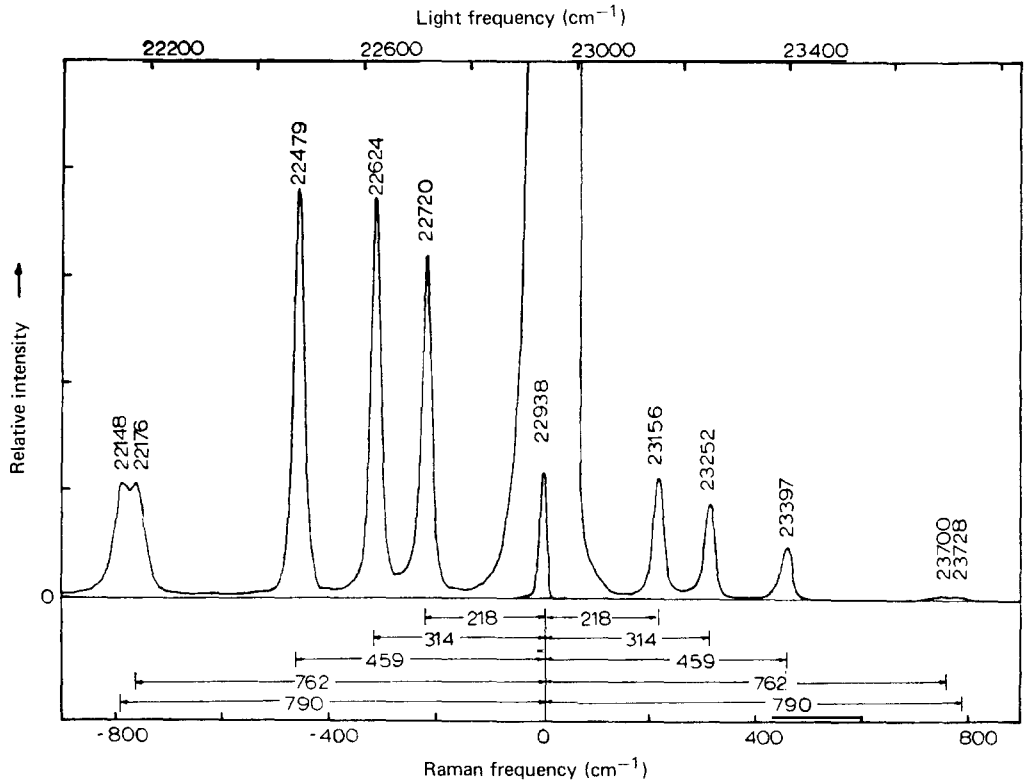

Fig. 2. Stokes and anti-Stokes lines in the Raman spectrum of CCl_4–mercury arc excitation, 435.8 mm (22938 cm^{-1}).

If all the shifts in frequency observed in the Raman corresponded to IR absorption bands, there would be very little practical interest in this technique. However, as previously noted, the two processes are governed by different selection rules involved with the electrical nature of the normal vibration and the oscillating electric field of the electromagnetic radiation. Infrared absorption occurs when the interaction of the molecule with the light produces a change in the dipole moment during a normal vibration. Raman scattering occurs when the molecular motion produces a change in the polarizability of the molecule.

These fundamental differences in the processes which govern infrared absorption and Raman scattering provide the basis for the appearance of bands or differences in band intensities in the spectra. This in turn facilitates the identification of various chemical groupings within molecules. The development of group frequencies in the Raman has already been of considerable value in the utilization of this tool in analytical applications.

The vibrational analysis of molecules, through the use of group theory, allows the calculation of the number and activity of Raman and infrared bands to be expected in the spectrum of a molecule. Some frequencies may appear in common, but as the molecular symmetry increases, the differences between the Raman and IR spectra also increase until mutual exclusion is attained for those molecules with a center of inversion. Thus the infrared and Raman spectra provide a most important tool for determining molecular structure.

Polarization data also supply additional information for identifying the types of normal vibrations. Symmetrical modes in a molecule will be polarized in the Raman and this is an important aid in assigning these modes in structural analysis.

3. Development of modern Raman instrumentation

The history of Raman spectroscopy has been greatly influenced by developments in the available instrumentation. Most aspects of this history are well known, leading up to the production of commercial laser excited Raman spectrometers with high quality double monochromators, photomultiplier tubes, and photon counting in the early 1960's [3].

We are now in the period of a second generation of laser excited spectrometers, offering far greater potential for observation of weak spectra (all Raman spectra seem to fall in this class) than previously. Some aspects of this development were expected and have gradually become predominant. Others appeared quite unexpectedly.

It was probably inevitable that the helium–neon laser, with accompanying red sensitive photomultiplier tubes used in the early days of laser excited instruments, would give way to blue or green wavelength lasers. This has indeed been the case with virtually all Raman instruments now using argon or krypton ion lasers. Typical exciting wavelengths are shown in table 4. Even in this area, a recent development has been the availability of much higher laser powers up to 15 watt of cw power. It happens that very few condensed phase samples can withstand such power when focussed to a diffraction limited point, as is usual in Raman sampling. For certain cases, however, it is proving to be the difference between obtaining a spectrum and not obtaining one. This is particularly true for gas phase work.

A new photomultiplier tube is also part of this second generation instrument, featuring a Ga–As or multi-alkali photocathode surface. These tubes are typified by the RCA C31034 or the Hamamatsu 928. Two properties of these tubes make them desirable for Raman spectroscopy – – they have a high absolute quantum efficiency, and the response is constant over the entire visible spectrum. These properties are illustrated in fig. 3, where the RCA tube is compared to the ITT FW130 tube used in most instruments previously.

First generation laser excited instruments used gratings which were ruled. Now holographic gratings are available and this means a far more perfect grating. Since stray light rejection and throughput are of critical importance to Raman spectroscopy, the holographic grating has meant a significant improvement in signal to noise ratios. It has also improved performance in the low frequency region, close to the Raman exciting line. Of interest is the production of concave holographic gratings, in addition to the conventional plane gratings. A monochromator produced using these gratings requires no additional optical elements other than slits. This again reduces stray light. Such a monochromator is now commercially available [4]. The stray light rejection in these monochromators is sufficiently good that Raman spectra can be obtained with a single monochromator, rather than the double or triple monochromators used previously. While most spectroscopists are still using the double monochromator, it seems likely that more

Table 4
Laser emission wavelengths commonly used to excite Raman spectra

Lasing medium	Wavelength (s), nm
He–Ne	632.8
Ar^+	488.0
	514.5
Kr^+	530.9
	647.1

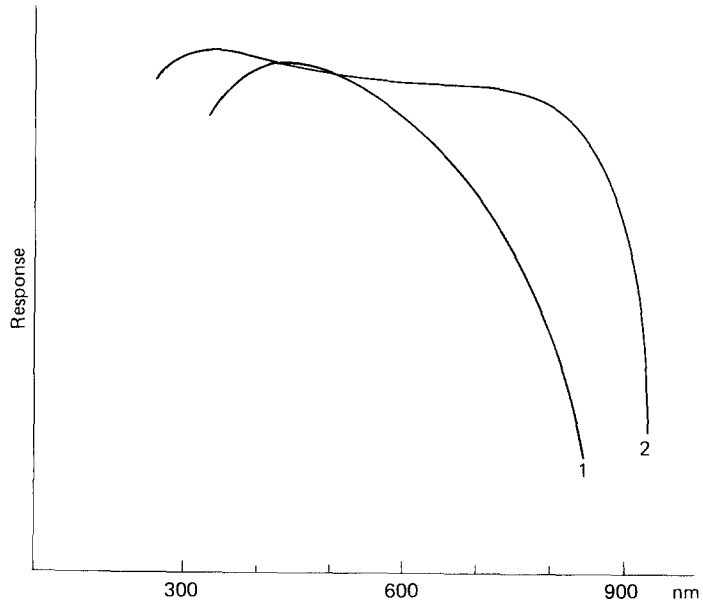

Fig. 3. Photomultiplier response curves in the visible region for (1) Extended S-20 response, such as ITT FW-130; (2) Ga–As photocathode, such as RCA C31034.

will begin to take advantage of the single monochromator to achieve higher throughput, even at the expense of a modest increase in stray light.

As one might expect, Raman instruments are being routinely interfaced to minicomputers and to microprocessors. Several articles have discussed strategies and implementation methods [5]. There are several reasons for doing this in Raman spectroscopy. Among these, signal averaging is foremost. Weak signals are readily enhanced by long integration times using the photon counting systems. The elimination of fluorescence by digital post processing of data is also possible [6]. This is being accomplished by computing the Fourier transform of the Raman spectrum, picking the proper Fourier coefficients to filter the broad fluorescent background from the Raman signal and recomputing the spectrum. Smoothing of data may also be accomplished in this way.

Polarization data, so important to applications of Raman spectroscopy, can also be readily extracted and displayed when data are available in digital form. One use of this is in separating the isotropic part of the polarizability, thus producing a display of only those modes belonging to the totally symmetric representation [7]. In a conventional Raman measurement, two spectra, referred to as $I_{\parallel}$ and $I_{\perp}$, are usually obtained. A depolarization ratio,

$$\rho = 3\beta^2/(45\alpha^2 + 4\beta^2) = I_{\perp}/I_{\parallel}$$

is then computed, where the α^2 terms are the isotropic portion of the polarizability, $\alpha = \frac{1}{3}(\alpha_1 + \alpha_2 + \alpha_3)$ and the β^2 terms are the anisotropic portion

$$\beta^2 = \tfrac{1}{2}[(\alpha_1 - \alpha_2)^2 + (\alpha_2 - \alpha_3)^2 + (\alpha_3 - \alpha_1)^2].$$

In the technique referred to above, $I_{\perp}$ is scaled by $\frac{4}{3}$ in the computer, then subtracted from $I_{\parallel}$ to produce a display proportional to 45 α^2. Scherer [7] first applied this to vibrational assignments. Later, Bulkin et al. [8] pointed out that for low symmetry molecules, structural questions often hinged on

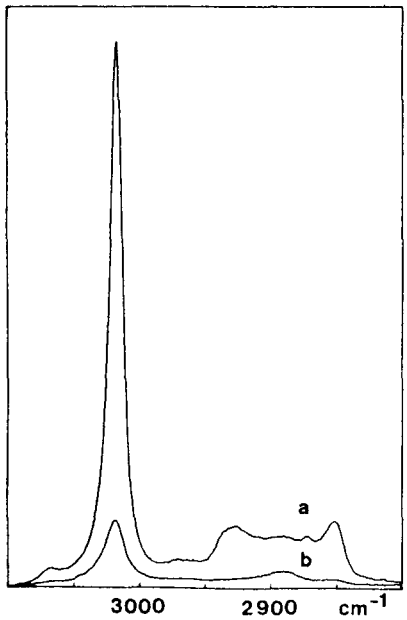

Fig. 4. Raman spectrum of dipalmitoyl lecithin in $CHCl_3$ solution at 3 cm^{-1} resolution: a, I_{vv}; b, I_{vh}. (From ref. [9].)

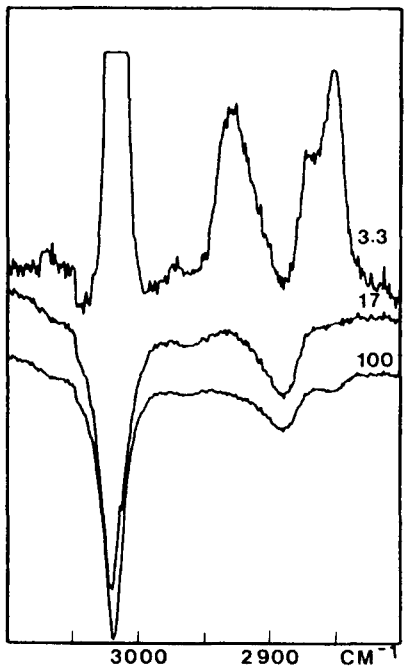

Fig. 5. Spectra computed from I_{vv} and I_{vh} spectra of fig. 4 using $1/\rho$ values as indicated. (From ref. [9].)

determining whether a molecule possessed C_s or C_1 symmetry. In the former case both polarized and depolarized bands should be observed; in the latter case only polarized. The polarizability separation technique is a convenient check on this. The relationship of polarization to structure will be discussed at length in a later section of this paper.

Krishnan and Bulkin [9] have shown that if the scaling factor is greater than $\frac{4}{3}$, bands of any depolarization ratio may be removed from the spectrum, thus providing a means for effective resolution enhancement of data. They have also discussed some limitations of this technique. Fig. 4 shows a complex envelope with many unresolved components.

In each of the traces shown in fig. 5 a different value of $1/\rho$ is used to scale $I_\perp$. As can be seen, each subtraction eliminates different bands from the band envelope.

Many other data processing applications have been accomplished with computer interfaced spectrometers. All of the work on Raman band shapes discussed later requires this. The Raman circular dichroism spectroscopy also requires digital data acquisition to be practical. Finally, to get good Raman intensity measurements, it is necessary to make a number of corrections to observed intensities. These have been discussed by Scherer [10]. They are readily applied to an entire spectrum by digital post multiplication.

4. Techniques

4.1. Sample handling

At times the advantage of Raman spectroscopy over other analytical techniques lies in the ease of examining small, intractable, or difficult-to-handle samples in a relatively short time. Raman spectra can

easily be run of gases, liquids and solids. There has not been quite as much done with the gaseous states because of the requirement for higher-powered lasers and more complex sampling apparatus. However, special gas-handling cells and devices are available and have been described in the literature [11].

Liquids are extremely easy to examine by Raman. Glass sample bottles, flasks, and ampoules can be used directly if the glass itself does not contain impurities which cause fluorescence. The most common liquid devices, however, are 1.5 mm od capillary tubes in which samples are run neat or with solvents such as CCl_4 or CS_2. Water, an opaque solvent for IR work, is a poor scatterer and is used frequently for Raman measurements.

Solid state sampling is also simple and straightforward in the Raman. Samples can be tamped into an open-ended cavity for front surface illumination using a 180° mount platform or into a glass capillary tube for transverse excitation. Fibers, block specimens, and films can be studied directly without any special preparation. Minimum size of such samples is determined by the size of the focussed laser spot and the difficulty of mounting the sample. Potassium bromide pellets mounted at 45° to the incident laser beam are also used quite frequently for Raman spectra of solid state samples.

4.2. Micro work

The size of the laser beam allows the Raman spectra of small volumes of gases or liquids to be examined.

Freeman and co-workers [12] have routinely obtained spectra from 2 nl liquid. Nyquist and Kagel [13] have gotten useful spectra from as little as 0.1 nl liquid in a 50 μm capillary. Rosasco and Simmons [14] have done experiments running Raman spectra of gases contained in glass bubbles where the effective scattering volumes were in the sub nl range. Barrett and Adams [15] have also reported the Raman spectra of O_2 and other gases from jets issuing from a nozzle in the 0.01 nl range.

4.3. The Raman microprobe

One of the most interesting developments in the application of Raman spectroscopy to microchemical problems has been the coupling of a microscope to the Raman spectrometer [16–20]. This allows one to examine a surface spectroscopically so as to discover non-uniformities which may be present and elucidate their chemical nature.

A schematic diagram of the commercially available Raman microprobe called MOLE (Molecular Optics Laser Examiner) is shown in fig. 6. In this system, the laser beam can be scanned over the sample surface or positioned to any point on the surface. The beam is approximately 1 mm^2.

Two modes of operation are possible. In the point mode, an area of interest on the surface is selected using the light microscope. The laser beam is positioned to this point and a spectrum is obtained.

In the global mode, the spectrometer is set to a particular frequency characteristic of a species of interest and the beam is scanned over the surface. Using vidicon readout the two dimensional spatial distribution of Raman scattering at the given wavenumber is determined.

One of the major applications of the Raman microprobe thus far has been to study inclusions in minerals. Particular inclusions can be isolated using the light microscope, then their spectra obtained in the point mode. Alternatively, in a sample with many diverse inclusions, the global mode can be used to construct a map of the surface.

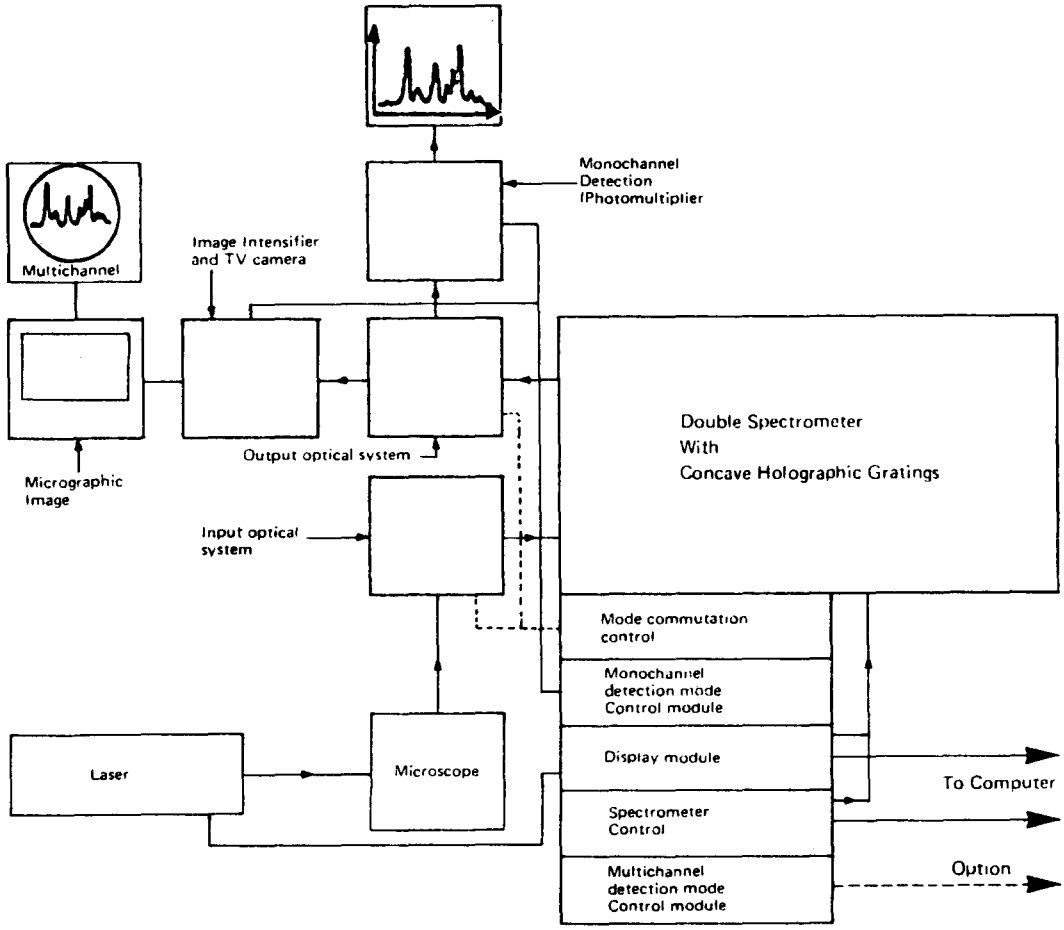

Fig. 6. Schematic diagram of the Raman microprobe commercial instrument manufactured by Instruments SA. For discussion see text.

Fig. 7 shows one example illustrating the modes of operation of the Raman microprobe. In the upper left frame, three particles are seen by the light microscope in the field of view. These give the composite Raman spectrum seen at the upper right. Individual particles can be isolated by the light microscope and their spectra obtained in the point mode. These spectra can be used to identify the particles as TiO_2 and $SrSO_4$. By setting the spectrometer in the global mode to the frequencies indicated by arrows in the figure, the images at center and lower left are obtained.

There are many types of samples to which the microprobe can be applied, including organic and inorganic species, polymers, salts of organic acids, and materials of biological importance such as urea and cholesterol [17]. Vibrational spectra have also been obtained from individual microcrystals and fibers of sheet and chain silicate materials such as tremolite and talc [21].

The Raman microscope has applicability in fields such as air pollution research, where the characterization of particulates is important. Fig. 8 shows the spectrum of an actual dust particle from urban air particulates. The particle was identified as $CaSO_4$ (anhydrite) from comparison of the major bands with a spectral reference. The broad bands at ~1400 and 1600 cm^{-1} have been attributed to degraded organic compounds or soot coating [22].

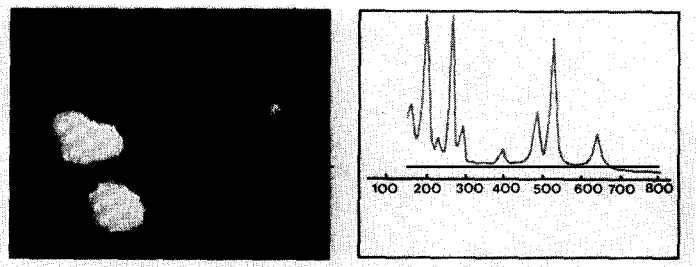

A sample is placed on the microscope slide and photographed (left). On the right is the total Raman spectrum obtained from the total field of view. Particles on the left are anatase (TiO_2); particle on the right is celestine ($SrSO_4$). Because the sum of the two spectra shown below is identical to the above total spectrum, there are no other chemical compounds present.

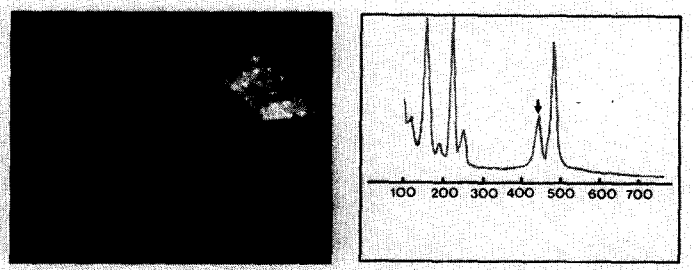

The laser light scattered from the particle on the right is analyzed for Raman spectrum to yield the partial spectrum shown at right. Image at left was obtained by setting the spectrometer for light at the frequency indicated by the arrow on the spectrum.

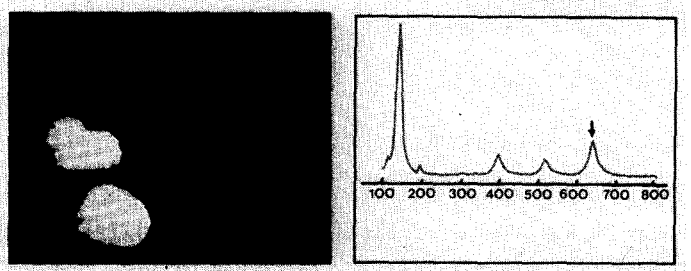

The laser light scattered from the two particles on the left is analyzed for the Raman spectrum shown at right. Image at left was obtained by setting spectrometer for light at the frequency indicated by the arrow on the spectrum.

Fig. 7. Illustration of the use of the Raman microprobe.

4.4. The rotating cell

Rotating cells were originally developed by Kiefer and Bernstein [23–24] to study deeply colored, highly absorbing materials which otherwise would be destroyed by intense localized overheating caused by the laser. Cell designs have undergone many modifications [25–27], and their applications to problems involving liquids [23], solids [24, 28, 29] and gases [30] have grown tremendously.

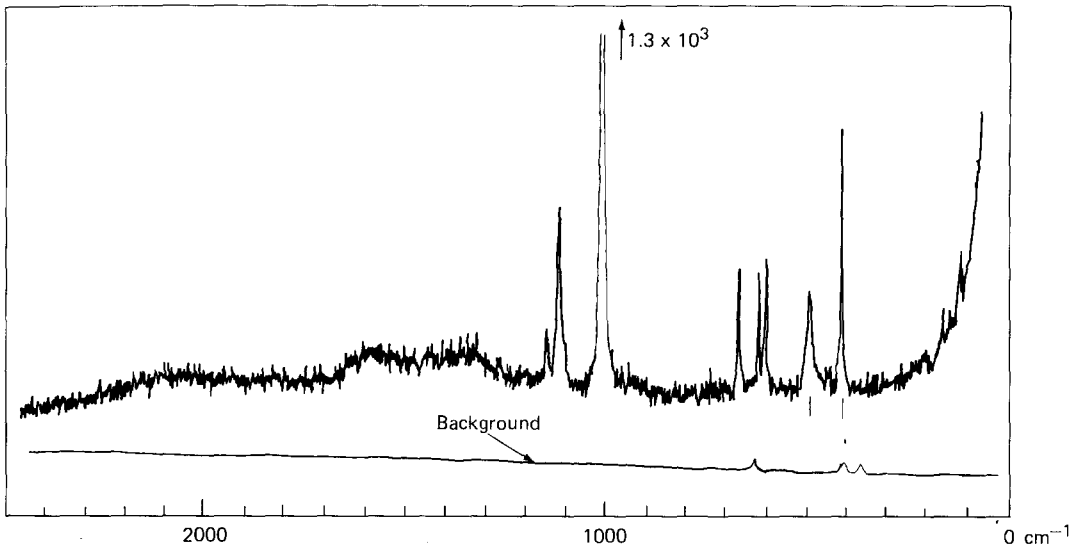

Fig. 8. Raman microscope spectrum of 8 μm particle from urban dust on Al_2O_3 substrate. (From ref. [17].)

The rotating cell is also a useful device for studying semi-micro samples [31]. Fig. 9 shows the Raman spectrum of 1.0 mg of $KMnO_4$ evaporated on a rotating sample holder from aqueous solution. Not only are the ν_1 and ν_3 bands at 840 cm^{-1} and 920 cm^{-1} observable (fig. 9A), but so are the second and third overtones and combinations (figs. 9B and 9C).

The rotating cell technique has also been adapted to record difference spectra of binary liquid systems using a divided cell and a gated electronic system [32]. Unwanted solvent bands can thus be eliminated from the spectrum of a solution. Fig. 10 shows a 1:1 mixture of CCl_4 (A) and $CHCl_3$ (B) compared to the pure liquids. The upper field shows the Raman spectrum of the mixture (A + B); the second field shows the Raman spectrum of the reference liquid CCl_4 (−A) while the middle field displays the difference Raman spectrum of the mixture vs. the reference liquid [(A + B) − A]. Spectrum −B in fig. 10 is the reference liquid $CHCl_3$, and the lower field shows the Raman difference spectrum of the mixture when $CHCl_3$ is the reference liquid. This difference Raman technique has also allowed

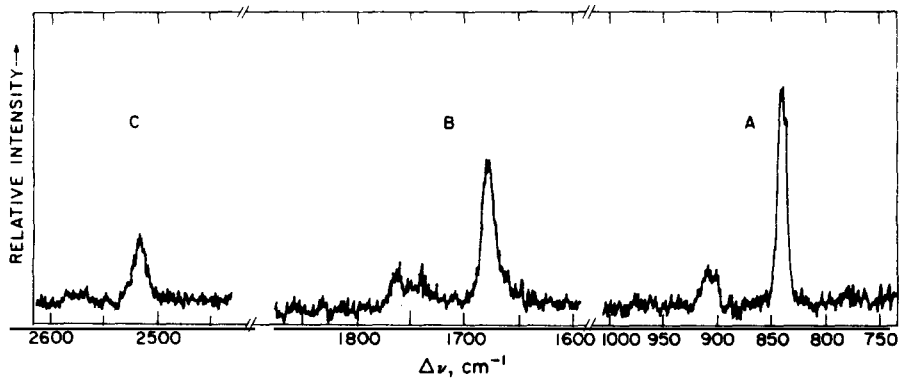

Fig. 9. The Raman spectrum of 1.0 mg of $KMnO_4$ evaporated on a rotating sample holder from aqueous solution. (From ref. [31].)

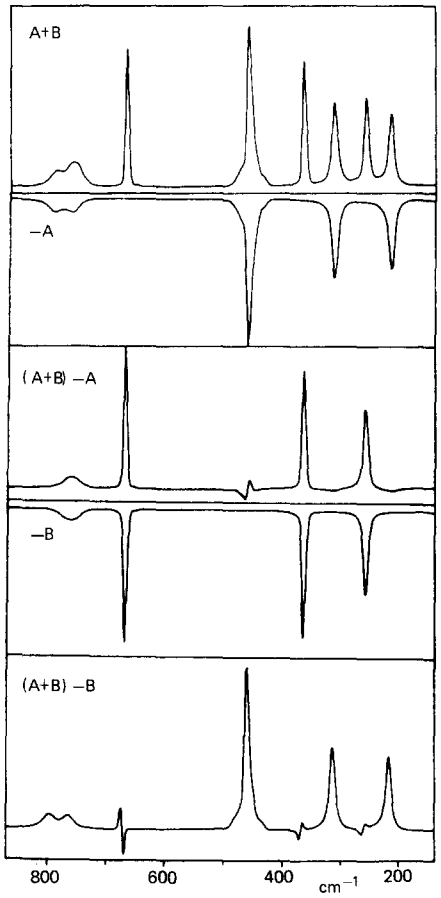

Fig. 10. Raman and difference Raman spectra of CCl_4 (A), $CHCl_3$ (B) and a mixture of CCl_4 and $CHCl_3$ (A : B = 50 : 50 vol. %); see text. (From ref. [32].)

accurate wavenumber shift measurements and corrections of the intensity error of Raman lines obtained from highly absorbing solutions [32].

Difference spectra can be applied to solids as well as liquids by modification of a rotating solid sample cell [27]. Bodenheimer et al. [33] have applied this technique to the study of single crystals under various orientations.

4.5. Quantitative analysis

Raman spectroscopy can be used for quantitative work as well as qualitative studies and there are many different methods of doing this. Usually internal standards are added to unknowns or bands are selected for reference which are unaffected by compositional changes [34–37], but Turner [38–39] obtained good quantitative results with 10 mm fluorimeter cells in a cell replacement method.

Ratioing techniques have also been used quite successfully. Wancheck et al. [40] reported a ratio method for determining the concentration of unreacted styrene monomer in latexes from an emulsion batch process for producing styrene/butadiene rubber. The latex samples were examined in melting point capillary tubes. Fig. 11 shows the C=C stretching region in the Raman spectrum for a standard

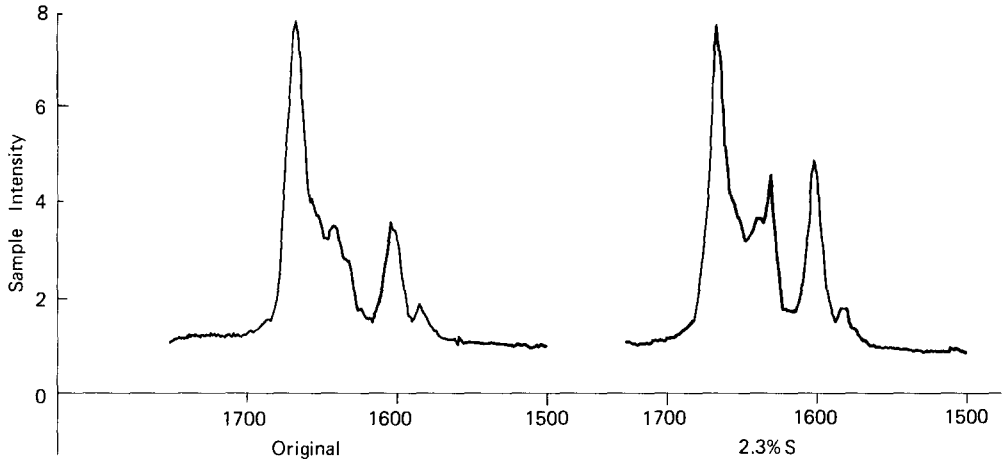

Fig. 11. Addition of styrene to styrene/butadiene latexes. (From ref. [40].)

latex sample containing 0.6 wt % residual styrene monomer as measured by liquid chromatography and spiked with styrene to a total concentration of 2.3 wt %. The typical polybutadiene peaks at 1640 cm^{-1} (1,2-vinyl), 1652 (cis-1,4), and 1668 cm^{-1} (trans-1,4) are present plus the aromatic ring vibration of polystyrene at 1600 cm^{-1}. The styrene monomer peak occurs at 1632 cm^{-1}. As a general rule in free radical polymerization of butadiene, the 1,4 mode of addition predominates and the trans/cis ratio is determined by the polymerization temperature. For the commercial and experimental high butadiene latexes examined, there was little cis or 1,2-vinyl polymer, but more importantly, the distribution of unsaturated structures did not vary as determined by IR and NMR. Therefore, an analytical method was established which used the ratio of the 1632 cm^{-1} free styrene band to the 1668 cm^{-1} trans 1,4 polybutadiene band.

Calibration points were prepared by standard addition techniques of styrene monomer over the range 0.6 to 12.4 wt % styrene. The values of residual styrene obtained by the Raman technique were confirmed initially by liquid chromatography. The agreement between these methods was ±0.3% and reproducibility on samples by the Raman method was ±0.1%.

The ability to examine water solutions directly was important in an industrial application where polymer plant personnel requested information on the extent of hydrolysis of acrylonitrile in a recycle monomer [41]. Acrylonitrile is known to hydrolyze slowly in water and to study this hydrolysis a capillary tube containing a 5% solution of acrylonitrile in water was monitored by Raman spectroscopy for a period of 29 days. Fig. 12 presents the data. The two hydrolysis products are hydracrylonitrile and acrylamide. Both of these could be followed quantitatively in samples from the plant with no more effort involved than filling a capillary tube and utilizing 20 minutes of Raman instrument time per day.

The band ratio technique has also been successfully employed to determine the composition of copolymers [6]. Fig. 13 is the calibration curve for determining composition of acrylonitrile/styrene copolymers. In this case the Raman was calibrated against NMR and C, H, N elemental analyses for a set of standards. Subsequent Raman results on actual samples could be obtained very rapidly.

Fig. 14 is another illustration of quantitative Raman spectroscopy. Without any special cells or techniques benzene can be detected easily in carbon tetrachloride at concentration levels down to at least 110 ppm [42].

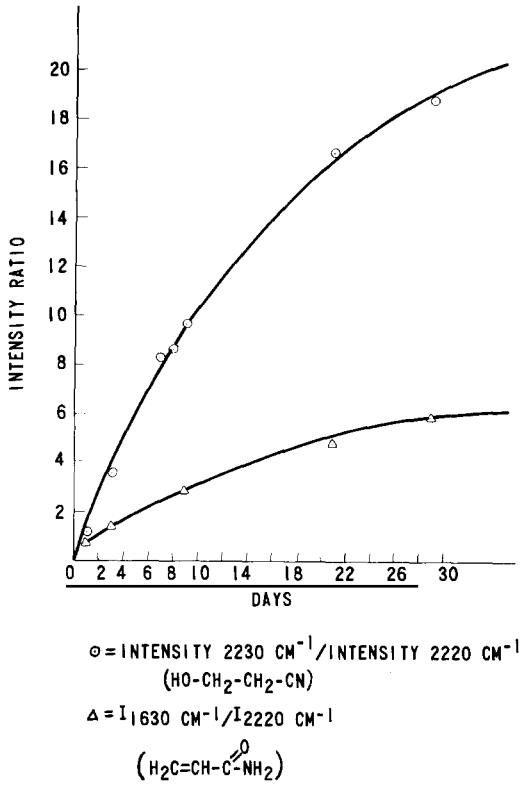

Fig. 12. Acrylonitrile hydrolysis study. (From ref. [41].)

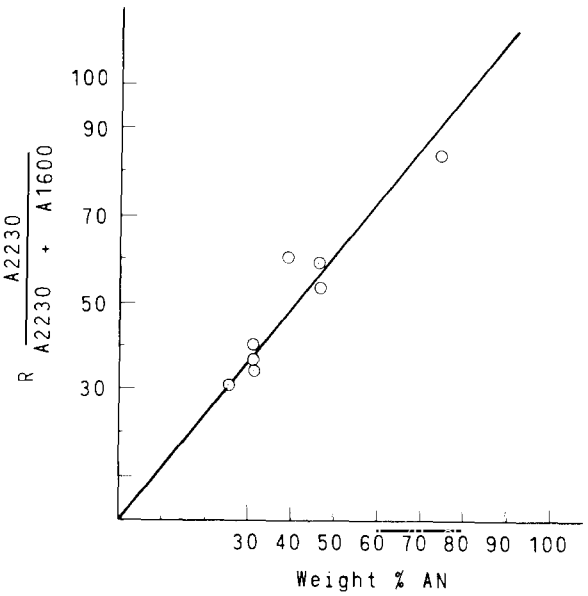

Fig. 13. Calibration curve for acrylonitrile/styrene composition. (From ref. [6].)

A sample of ^{13}C-enriched $CHCl_3$ is shown in fig. 15, taken in the original manufacturer's ampoule [43]. The symmetric C–Cl stretching vibration near 670 cm^{-1} is split into two components which are assigned to molecules with ^{12}C and ^{13}C atoms respectively. The relative peak heights of these two bands gives a ^{13}C content of 58.7%.

Quantitative Raman spectroscopy has also been applied to the determination of oxyanion impurities in reagent grade chemicals such as $NaNO_3$ [44]. In this instance integrated band intensities as measured by a planimeter were used.

The rotating cell technique mentioned previously has also been utilized for quantitative work. A rotating cylindrical double cell with separate compartments for sample and reference obviates the need for an internal standard. This type of rotating cell has been used successfully with mixtures of carbon tetrachloride and toluene and on equilibrium studies of the dissociation of nitric acid [45].

4.6. Separated fractions

Raman spectroscopy is an ideal tool to use in combination with other separation methods such as gas, thin-layer, or liquid chromatography because of the ability to look at very small sample areas.

Since silica is a poor Raman scatterer, thin layer spots may be examined directly on a developed plate. Such a spectrum is shown in fig. 16 [6]. An evaporated gasoline sample was separated on a silica coated alumina strip and developed in 95% benzene/5% acetone. The spot was cut out, mounted on the

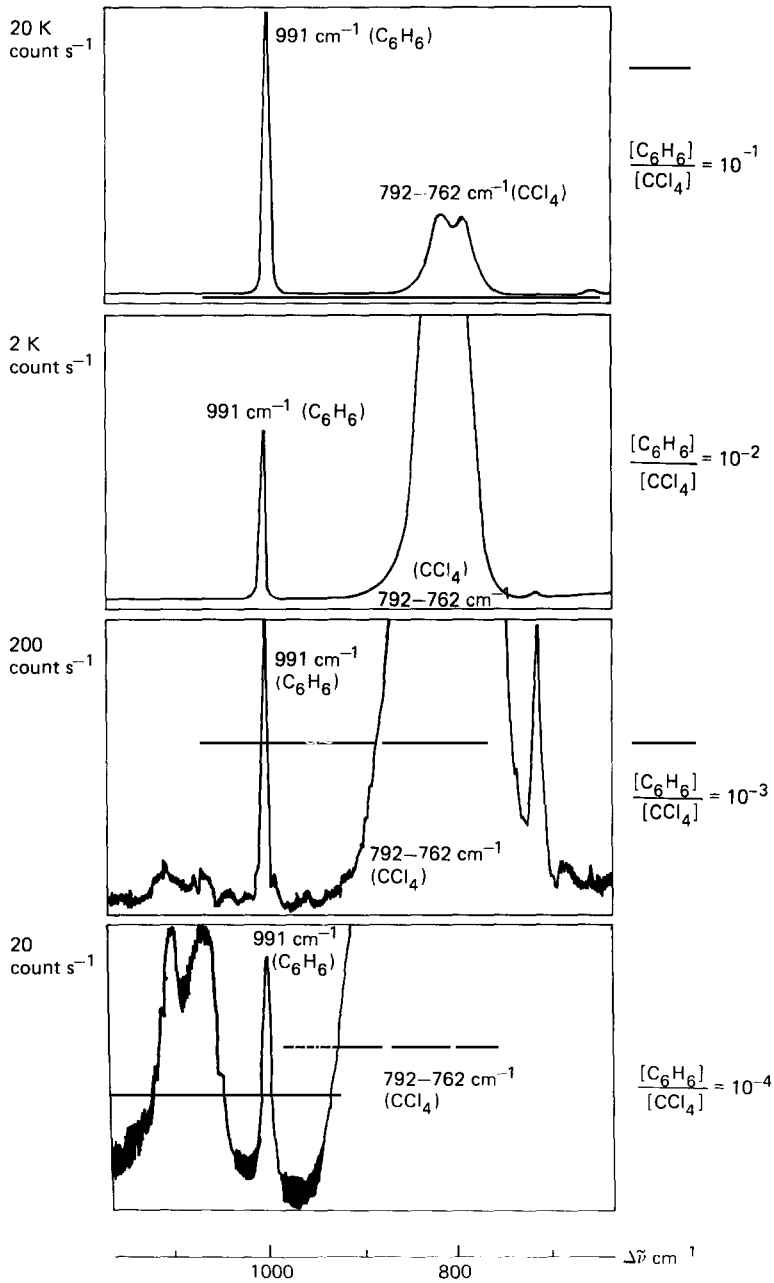

Fig. 14. Quantitative analysis of benzene in carbon tetrachloride, 488.0 nm excitation. (From ref. [42].)

180° viewing platform, and the laser focussed directly on the adsorbed layer by careful positioning of the microscope objective lens. Using the 514.5 nm argon ion line with 3 cm^{-1} slits, a spectrum easily identified as cresyl diphenyl phosphate was obtained. The ability to signal average spectra to improve sensitivity was also important. Huvenne et al. [46] have identified dodecane on silica gel plates by using a laser scanning technique in a back scattering geometry and data accumulation by a minicomputer.

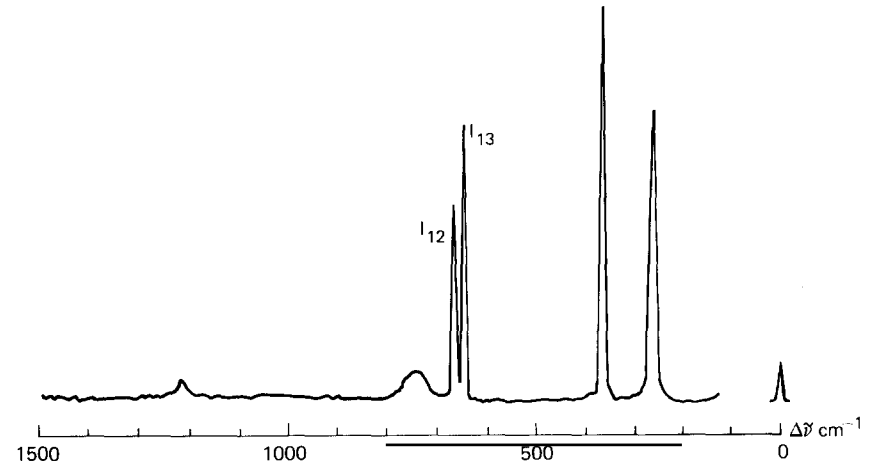

Fig. 15. Raman spectrum of chloroform, 57.6% labelled with ^{13}C in the original ampoule. (From ref. [43].)

Adams and Gardner [47] obtained the spectra of hexamethylene-tetramine and several substituted benzophenones in situ on thin layer plates. They found that success depended upon the nature of the substrate (Kieselgel HR was better than Supreme, a grade of china clay, or Rutile), the eluant, the retention factor, fluorescence of both plate and sample, and the scattering efficiency of the sample itself.

A simple technique has been developed for examining liquid chromatography fractions [6]. The collected peak is deposited stepwise under vacuum onto 15 mg of KBr. A 1.5 mm micro disc is prepared

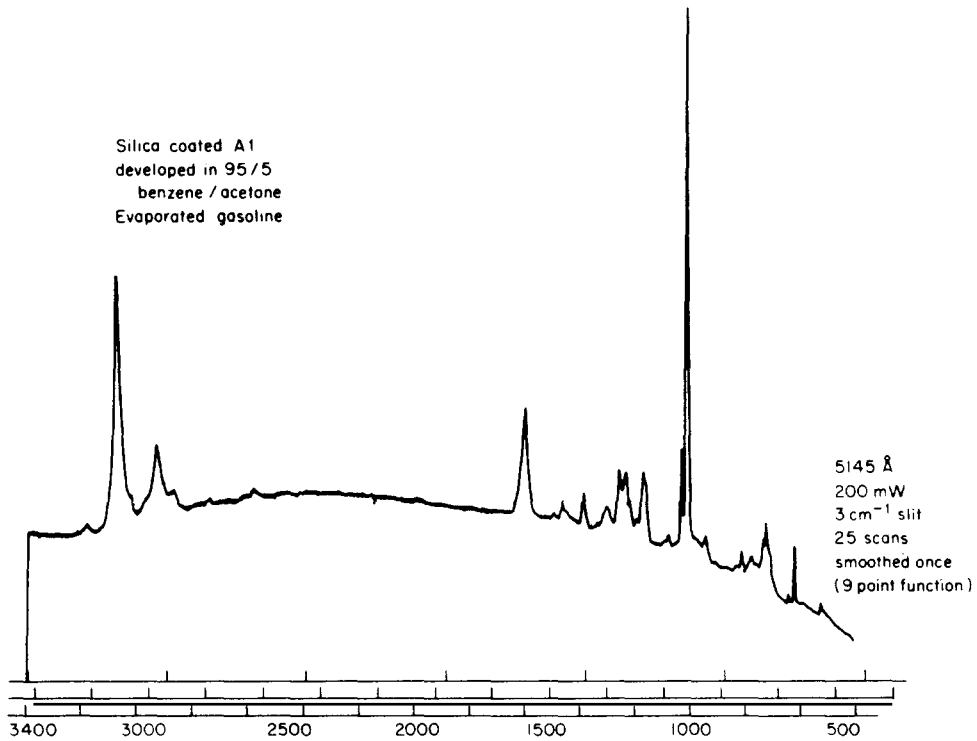

Fig. 16. TLC spot identified as cresyl diphenyl phosphate. (From ref. [6].)

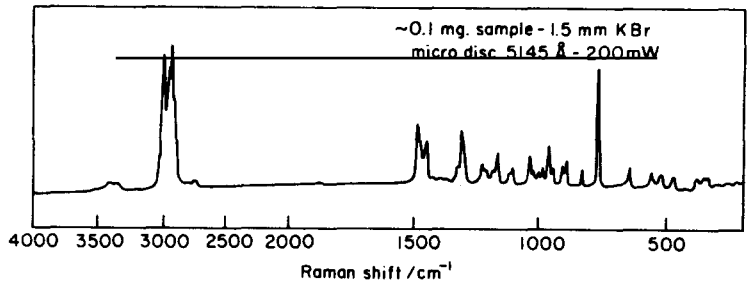

Fig. 17. Raman spectrum of a liquid chromatography fraction containing 100 μg of sample. (From ref. [6].)

and the spectrum is obtained with 180° viewing. Fig. 17 shows the spectrum of 100 μg of a processing aid separated from a commercial polymer by liquid chromatography. With computer solvent subtraction and signal averaging, Raman has the potential to examine LC fractions in glass vials with only minimal preconcentration.

Raman can also be used to characterize small quantities of samples trapped as GC effluents [48–49]. Fig. 18 shows a simple collection system consisting of a 0.3-mm id glass capillary inserted into a septum. Both ends of the capillary are open. When a peak appears at the detector, the capillary is held at the GC exit port with a cool moist tissue which condenses the liquid droplets along the walls. The walls can then be "swept" with a 0.1-mm id capillary to concentrate a slug of material at one end. This slug usually has a volume between 5 and 10 nl. The use of two different size capillaries permits a reasonable gas flow and yet allows small enough injections (2–5 μl) of sample to be practical.

A slightly different GC trapping system has been described by Nyquist and Kagel [50] in which the sample is centrifuged into a constriction in the capillary after being collected in a portion cooled by liquid nitrogen. Fig. 19 shows two spectra obtained from the GC trapping of tribromopropane cuts. The upper spectrum is that of 2 μl of 1,2,2-tribromopropane while the lower represents 20 nl of the 1,2,3-isomer. The isomer was less than 1% of the original sample and was completely undetectable by IR.

The obvious advantage of employing any of the separatory techniques in obtaining Raman spectra is that the separated portion only contains one component and is relatively free from fluorescing impurities.

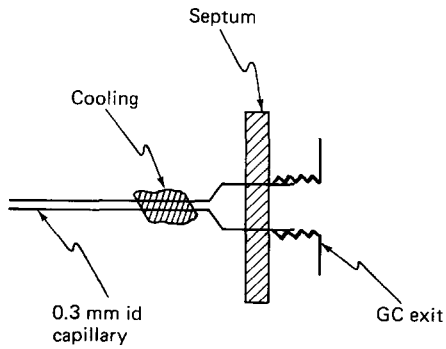

Fig. 18. Apparatus for collecting gas chromatograph effluents for Raman spectroscopy. (From ref. [48].)

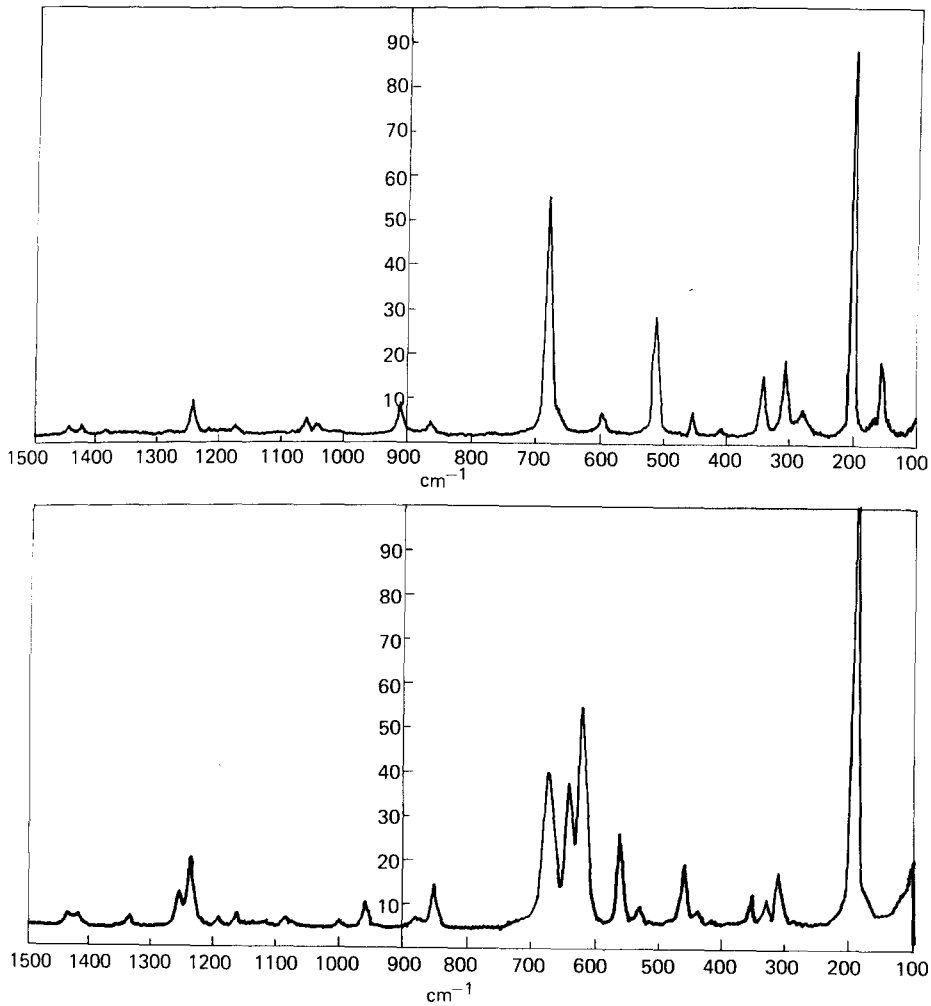

Fig. 19. Raman spectra of trapped GC fractions. Upper, 2 μl of 1,2,2-tribromopropane; lower, 20 μl of 1,2,3-tribromopropane. 632.8 nm He/Ne excitation. (From ref. [50].)

4.7. Resonance Raman

Resonance Raman occurs when an electronic absorption band is located near the exciting line of the laser. When this happens, the form of the spectrum may change and the intensity increases greatly. Fig. 20a,b shows the difference between the resonance Raman spectrum of K_2CrO_4 (solid sample taken in a rotating cell with 363.8 nm excitation) and the normal spectrum of K_2CrO_4 (aqueous solution obtained with 632.8 nm excitation). Fig. 20c is the absorption spectrum of K_2CrO_4 in aqueous solution. The normal Raman spectrum shows only the four bands of the CrO_4^{2-} ion. The resonance Raman spectrum shows the entire overtone series of the 853 cm^{-1} band. As the overtone series progresses, the bandwidth increases but the intensity decreases. The observation of the series allows the anharmonicity to be determined.

In addition to the anharmonicity another obvious use of resonance Raman, because of its intensity

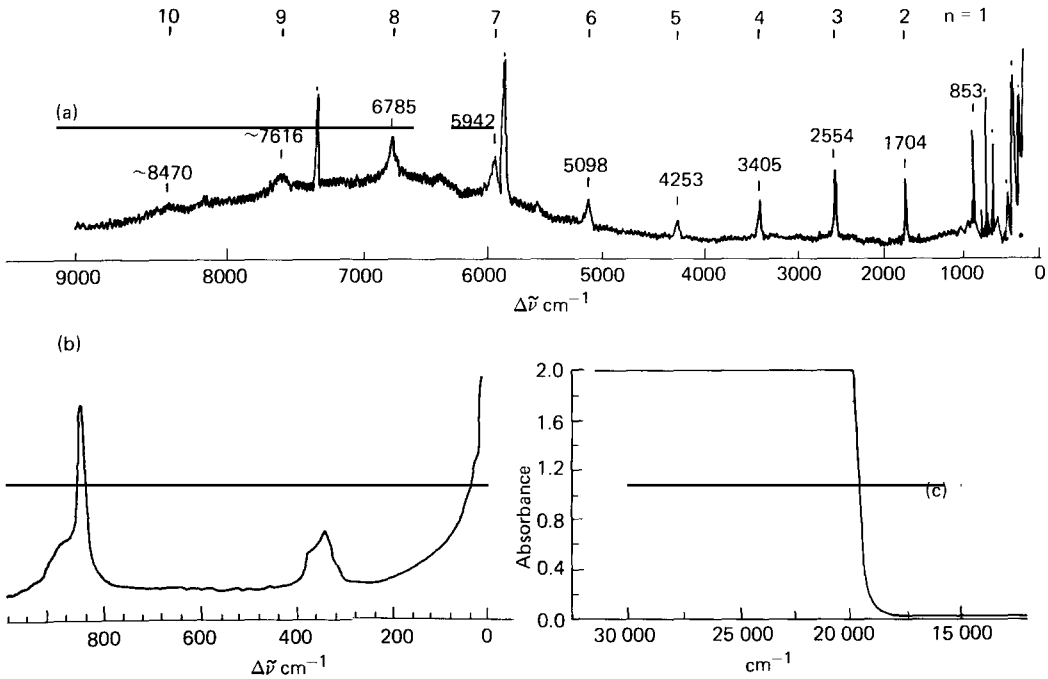

Fig. 20. (a) Resonance Raman spectrum of solid K_2CrO_4, 363.8 nm excitation, rotating sample cell; lines marked + are laser lines; (b) Normal Raman spectrum, 632.8 nm excitation, and (c) Absorption spectrum of K_2CrO_4, aqueous solution 1.0 M. (From H. J. Bernstein, in: Advances in Raman Spectroscopy, ed. J.P. Mathieu (Heyden, London, 1973) p. 312.)

enhancement, is to enable spectra of low concentrations to be obtained. Studies of matrix-isolated species have also been made [51]. Resonance Raman has been used extensively in biological studies for selective resonance enhancement in complex systems and thus has served as a subtle and sensitive probe in molecular structural and environmental studies. Examples will be given in later sections of this paper. The growing availability of a range of laser excitation frequencies and the development of tunable lasers will undoubtedly contribute to many more applications of this effect.

5. Group frequencies

In Raman as well as in infrared spectroscopy, characteristic frequencies are found which are useful in chemical applications of these techniques. Raman scattering occurs if a bond is polarizable; IR requires a change in dipole moment. For this reason, Raman is particularly informative about groups like –C–S–, –S–S–, –C–C–, –N=N– and –C=C–, whereas IR can be used to characterize groups like OH, C=O, P=O, S=O and NO_2. In most cases the IR and Raman data are complementary and it is helpful, even necessary, to have both for complete structural elucidation. In the past, IR group frequencies have been studied much more extensively [52–56], but many excellent texts and tables of Raman frequencies are now beginning to appear in the literature [43, 57–59]. Table 5 shows some characteristic bands which may be used for investigations using the Raman spectrum alone or a combination of Raman and infrared.

Raman is uniquely capable for characterizing many C=C stretching vibrations which generally occur

Table 5
Characteristic wavenumbers and Raman and infrared intensities of groups in organic compounds. (From ref. [2].)

Vibration[a]	Region (cm^{-1})	Intensity[b]	
		Raman	Infrared
ν(O–H)	3650–3000	w	s
ν(N–H)	3500–3300	m	m
ν(≡C–H)	3300	w	s
ν(=C–H)	3100–3000	s	m
ν(–C–H)	3000–2800	s	s
ν(–S–H)	2600–2550	s	w
ν(C≡N)	2255–2220	m–s	s–0
ν(C≡C)	2250–2100	vs	w–0
ν(C=O)	1820–1680	s–w	vs
ν(C=C)	1900–1500	vs–m	0–w
ν(C=N)	1680–1610	s	m
ν(N=N), aliphatic substituent	1580–1550	m	0
ν(N=N), aromatic substituent	1440–1410	m	0
ν_a((C–)NO_2)	1590–1530	m	s
ν_s((C–)NO_2)	1380–1340	vs	m
ν_a((C–)SO_2(–C))	1350–1310	w–0	s
ν_s((C–)SO_2(–C))	1160–1120	s	s
ν((C–)SO(–C))	1070–1020	m	s
ν(C=S)	1250–1000	s	w
$\delta(CH_2)$, $\delta_a(CH_3)$	1470–1400	m	m
$\delta_s(CH_3)$	1380	m–w, s, if at C=C	s–m
ν(CC), aromatics	1600, 1580	s–m	m–s
	1500, 1450	m–w	m–s
	1000	s (in mono-; *m*-; 1,3,5-derivatives)	0–w
ν(CC), alicyclics, and aliphatic chains	1300–600	s–m	m–w
ν_a(C–O—C)	1150–1060	w	s
ν_s(C–O–C)	970–800	s–m	w–0
ν_a(Si–O–Si)	1110–1000	w–0	vs
ν_s(Si–O–Si)	550–450	vs	w–0
ν(O–O)	900–845	s	0–w
ν(S–S)	550–430	s	0–w
ν(Se–Se)	330–290	s	0–w
ν(C(aromatic)–S)	1100–1080	s	s–m
ν(C(aliphatic)–S)	790–630	s	s–m
ν(C–Cl)	800–550	s	s
ν(C–Br)	700–500	s	s
ν(C–I)	660–480	s	s
δ_s(CC), aliphatic chains			
C_n, $n = 3, \ldots, 12$	400–250	s–m	w–0
$n > 12$	$2495/n$		
Lattice vibrations in molecular crystals (librations and translational vibrations)	200–20	vs–0	s–0

[a] ν stretching vibration, δ bending vibration, ν_s symmetric vibration, ν_a antisymmetric vibration.

[b] vs very strong, s strong, m medium, w weak, 0 very weak or inactive.

near 1640 cm^{-1} and are often weak in the infrared. In fact, when the band is symmetrically substituted, selection rules forbid any appearance of an IR band. It is this type of symmetrical vibration with symmetrical charge distributions which is very strong in the Raman.

Group frequency variations always occur systematically depending upon adjacent groups in a molecule. Thus, a study of these variations is also a study of the adjacent groups. The dependence of the C=C stretch frequency upon neighboring substituents is shown in table 6 and is especially evident in the cyclopropene derivatives. This is due to a vibrational coupling of adjoining bonds, not to a large change in bond force constants. When two oscillators of different frequencies are coupled the higher frequency will be shifted to higher values, the lower frequency to lower values; shifts are greater the closer the frequencies of the oscillators. Therefore, the ν(C=C) of cyclopropenes is shifted to lower frequencies when CH and CD groups are present and to higher frequencies when C–CH_3 is the adjoining group.

Another area where Raman has a distinct advantage over infrared is in the elucidation of the nature of sulfur bonding. SH, C–S and S–S vibrations have been studied extensively [50] and are quite well

Table 6
Characteristic wavenumbers of C=C double bonds in hydrocarbons and halocarbons (From ref. [2].)

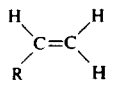	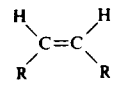	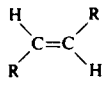	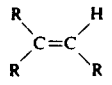	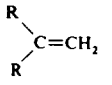
R = CH_3 1648 R = alkyl 1641	1669 1654	1681 1667	1672 1666	1658 1648
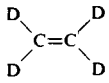	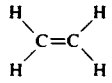	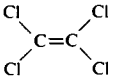	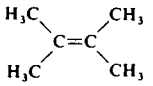	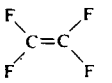
1515	1621	1571	1672	1672
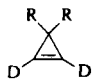	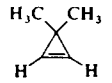	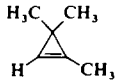	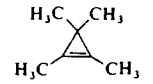	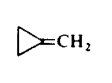
1525	1632	1768	1877	1780
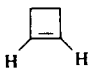	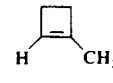	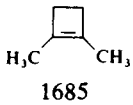	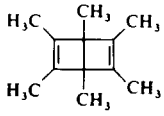	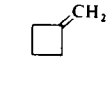
1566	1641	1685	1686	1678
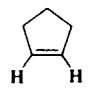	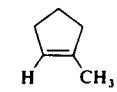	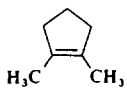	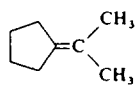	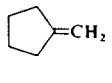
1614	1656	1685	1687	1657
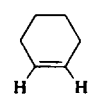	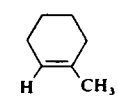	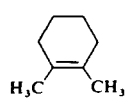	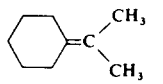	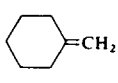
1649	1678	1685	1668	1651
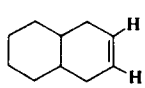	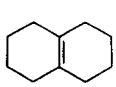	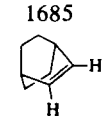	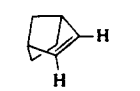	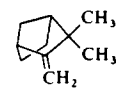
1650	1681	1614	1570	1672

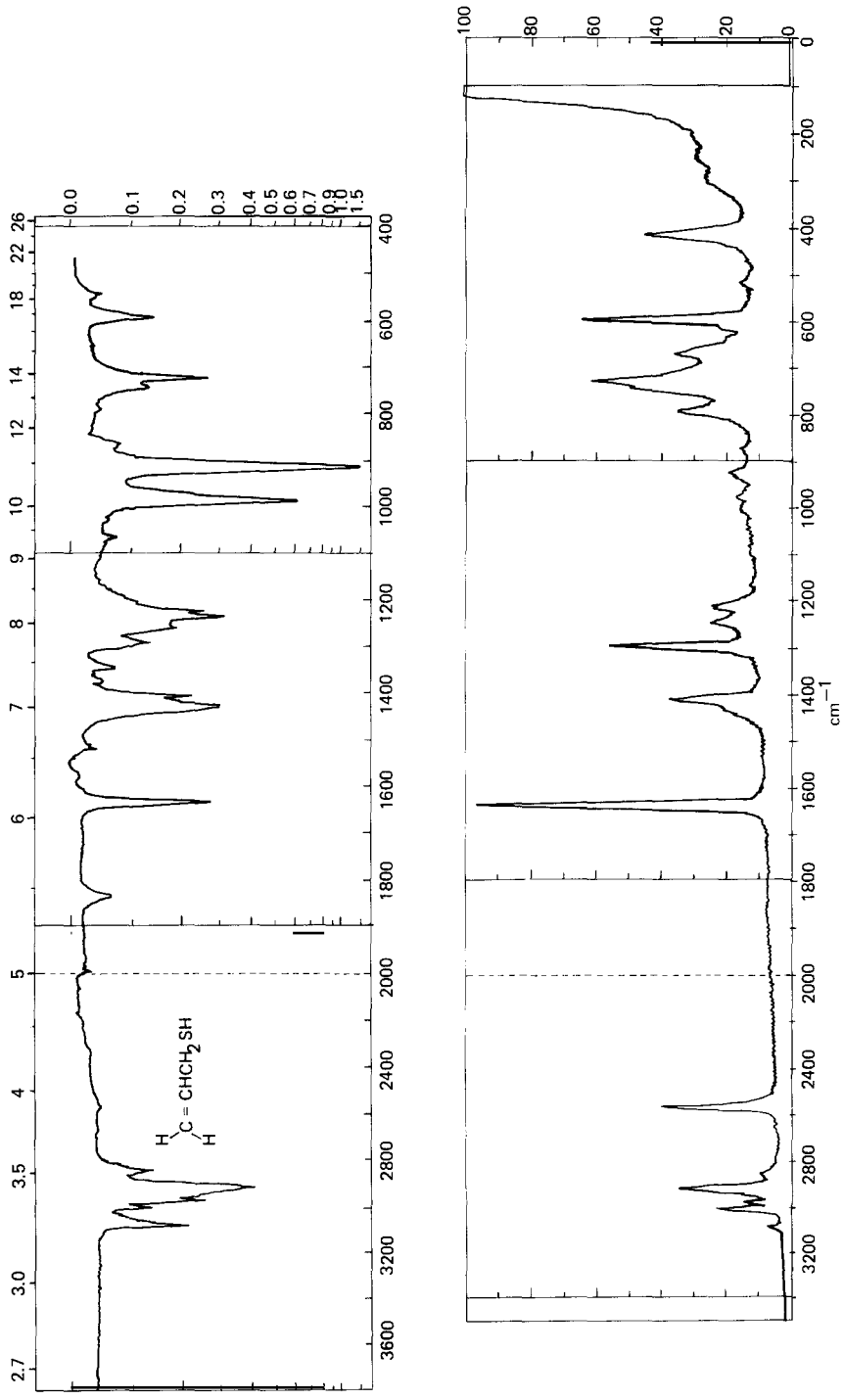

Fig. 21. Allyl mercaptan. Upper, IR spectrum, 10% in CCl_4 solution (3800 to 1333 cm^{-1}) and 10% in CS_2 solution (1333 to 4500 cm^{-1}). Solvents are compensated; lower, Raman spectrum, neat liquid. (From ref. [50].)

Table 7
Raman C–S, SH and S–S vibrations

Organomercaptans (SH stretching)		Organomercaptans (C–S stretching)	
R–SH	2575–2584	CH_3–S	705–785
HS–R–SH	2566–2582	RCH_2–S	660–670
		R_2CH–S	600–630
		R_3C–S	600–570
		HS–R–SH	613–729

Organosulfides (C–S–C stretching)		
	Asym	Sym
R–S–R′	696–782	641–696

Organodisulfides (S–S stretching)	
R–S–S–R′	501–546

defined. The SH stretch at ~2580 cm^{-1} is weak in the IR but quite intense in the Raman as shown in the spectra of allyl mercaptan, fig. 21. Also intense in the Raman are C–S vibrations occurring between 570 and 785 cm^{-1} which often appear as doublets or multiple bands due to the presence of rotational isomers. Organic sulfides exhibit both symmetric and antisymmetric C–S–C stretching vibrations in the region 570 to 800 cm^{-1}.

The antisymmetric C–S–C band is sometimes difficult to assign because it occurs in the same region as the CH_2 rocking vibration of aliphatic hydrocarbons and because there are sometimes multiple bands due to rotational isomers.

Organo disulfides generally have less complex spectra in the 700 to 800 cm^{-1} region than the corresponding organosulfides. There is no coupling between the in- and out-of phase –C–S–S–C– stretching vibrations and only one band appears. The –S–S stretching band occurs between 500 and 550 cm^{-1}.

Table 7 summarizes the Raman frequencies of the C–S, S–S and S–H vibrations. More detailed charts and discussions concerning the various sulfur-containing groups can be found in Nyquist and Kagel [50].

5.1. Carbon halogen stretching

Carbon halogen stretching bands occur between 1000–450 cm^{-1} in the Raman. In open-chain, mono-halogenated compounds, the stretching vibrations actually occur within the range 800–450 cm^{-1}. Once again, identification based on either the Raman or IR alone is unreliable. Many classes of compounds give strong IR bands (aromatics, alkynes, etc.) or strong Raman bands (branched alkanes, sulfur containing groups) in this same region, whereas ν(C–X) shows strong bands in both spectra. Evaluating both the IR and Raman spectra, it is possible to distinguish the halogen atoms and to detect the type of substitution present on the carbon atom attached to the halogen [60] (fig. 22).

Comparison of corresponding C–F, C–Cl and C–Br vibrations in similar compounds show that the intensity increases progressively from C–F to C–Br which is exactly the reverse of the IR. This behavior is predictable though, because it becomes easier to distort the electron cloud about the C–X through the series C–F to C–I, while the dipole moment decreases through the same series.

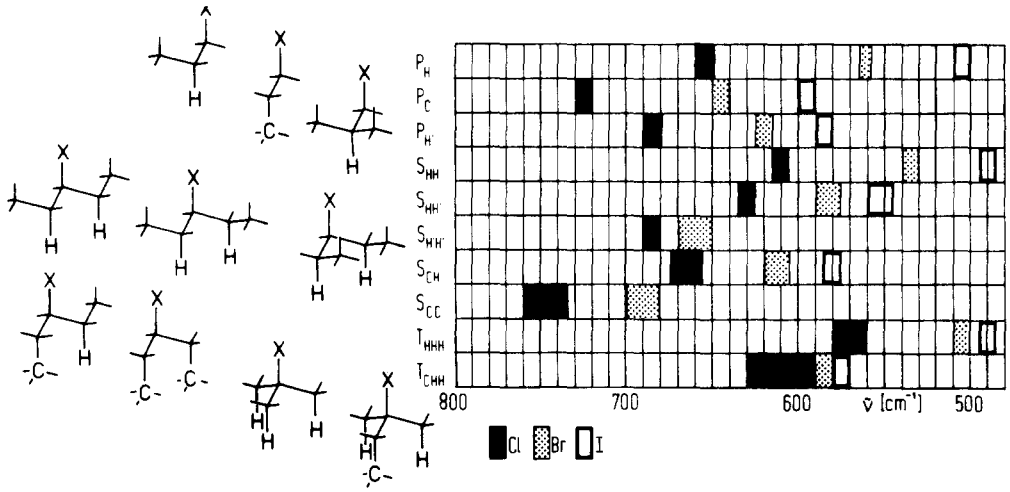

Fig. 22. Correlation between carbon-halogen stretching frequency and the type of substitution present on the adjoining carbon atom. (From ref. [60].)

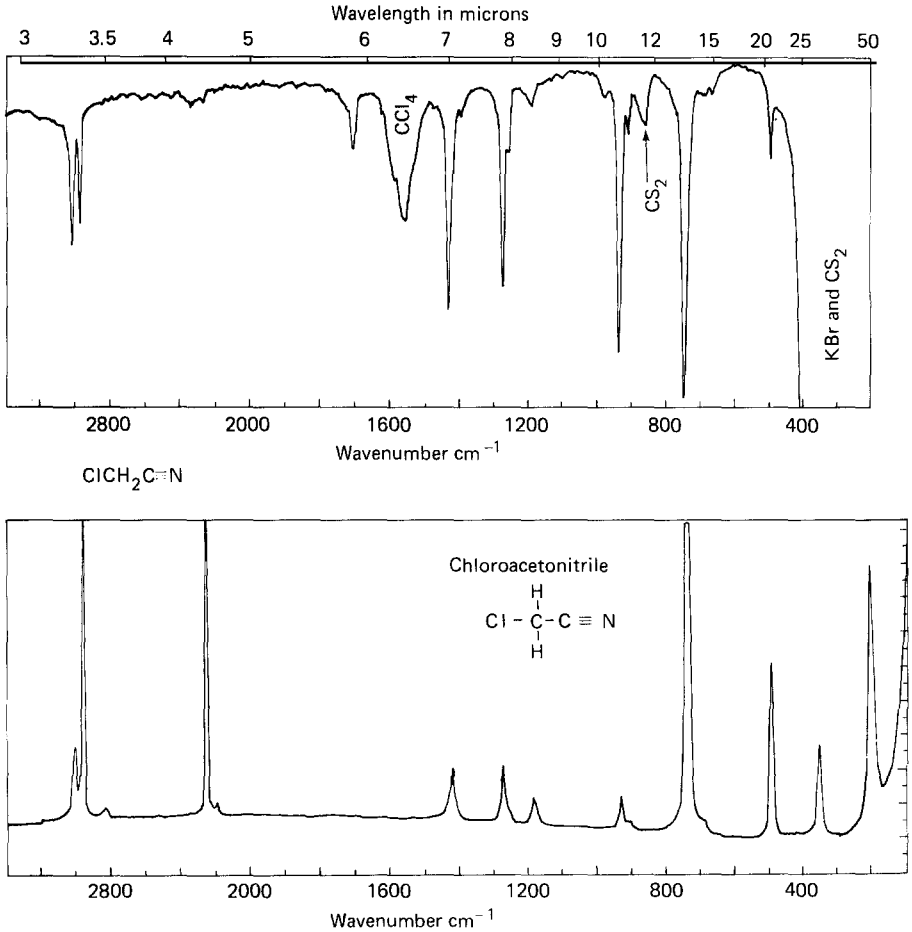

Fig. 23. Infrared and Raman spectra of α-chloroacetonitrile. Due to α-carbon halogenation, intensity of –C≡N stretch is drastically reduced in the IR but retained in the Raman. (From ref. [61].)

5.2. Triple bond stretching, C≡C and C≡N

The IR C≡C vibration near 2200 cm^{-1} is weak unless directly substituted with a polar group or atom, but the Raman vibration is always intense. Likewise, the C≡N vibration is variable in the IR but is always strong in the Raman. In fact, if the C≡N group is α-substituted with a strong electronegative group such as chlorine, the IR shows little or no C≡N absorption near 2250 cm^{-1} [61]. This is evident in the spectrum of α-chloroacetonitrile shown in fig. 23. However, the Raman spectrum shown in the same figure has a very intense C≡N bond. Thus it is more reliable to determine the presence or absence of both C≡C and C≡N with Raman than IR.

5.3. Aromatic structures

Raman is also extremely useful in the identification of aromatic structures. IR has classically been used for this purpose, because there are several regions of the spectrum with well-known characteristic absorptions. The CH stretching region above 3000 cm^{-1}, the overtone and combination bands in the 2000–1600 cm^{-1} region, the ring deformation bands in the 1500 and 1600 cm^{-1} regions and the out-of-plane hydrogen deformation and ring puckering modes in the 900–700 cm^{-1} region indicate the type of substitution. Monosubstituted aromatic compounds typically show the latter absorptions at 750 cm^{-1} and 700 cm^{-1} in the IR, but the presence of electron-withdrawing groups on the ring can significantly disturb or alter these vibrations. In the Raman the characteristic ring modes are not affected by these substituents and it is easy to identify a monosubstituted benzene ring by the following absorptions:

CH stretch near 3060 cm^{-1}
ring stretch doublet near 1600 cm^{-1}
ring in-plane bending 618 cm^{-1}
in-plane CH deformation 1028 cm^{-1}
in-plane ring deformation { 1000 cm^{-1} / sh 995 cm^{-1}.

Although not quite as definitive, other types of substituted benzenes also show well-resolved Raman absorptions. They are summarized in fig. 24. Dollish, Fateley and Bentley have discussed all of these bands more thoroughly [57].

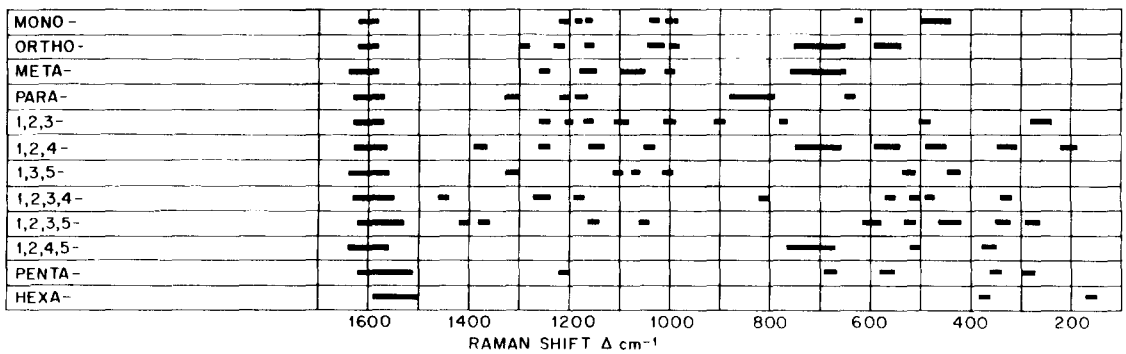

Fig. 24. Characteristic frequencies in the Raman spectra of substituted benzenes. (From ref. [57].)

5.4. Other characteristic vibrations

Some groups can *only* be identified by Raman spectroscopy. For example, there are no characteristic IR group frequencies for Se–Se, S–S and O–O. The O–O absorption, which gives rise to a strong band in the Raman near 700–900 cm^{-1} can be very useful for the identification of peroxides, peracids and peresters [43, 62].

Other groups such as C=O, N=N, C=N, NO_2, SO_2, NH and OH are seen in both the Raman and IR, and intensities, as well as the presence or absence of a band, can be used to aid in structural elucidation. In addition to the C-halogen already mentioned, the intensities of groups like X–H, OH and C–H are often the opposite of the IR.

Since complete molecular structure determinations can be made only by using both IR and Raman data, several authors have attempted to integrate the two [43, 59, 61].

6. Raman applications to organic chemistry

6.1. Structure elucidation

Both the IR and Raman spectra of a molecule are widely used in organic chemistry for structure elucidation. The differences in relative intensities of the various functional group peaks between the IR and Raman have already been noted. (The more unsymmetrically substituted a given bond, the greater the IR intensity and the weaker the Raman. Conversely, the more symmetrically substituted the groups, the stronger the Raman.)

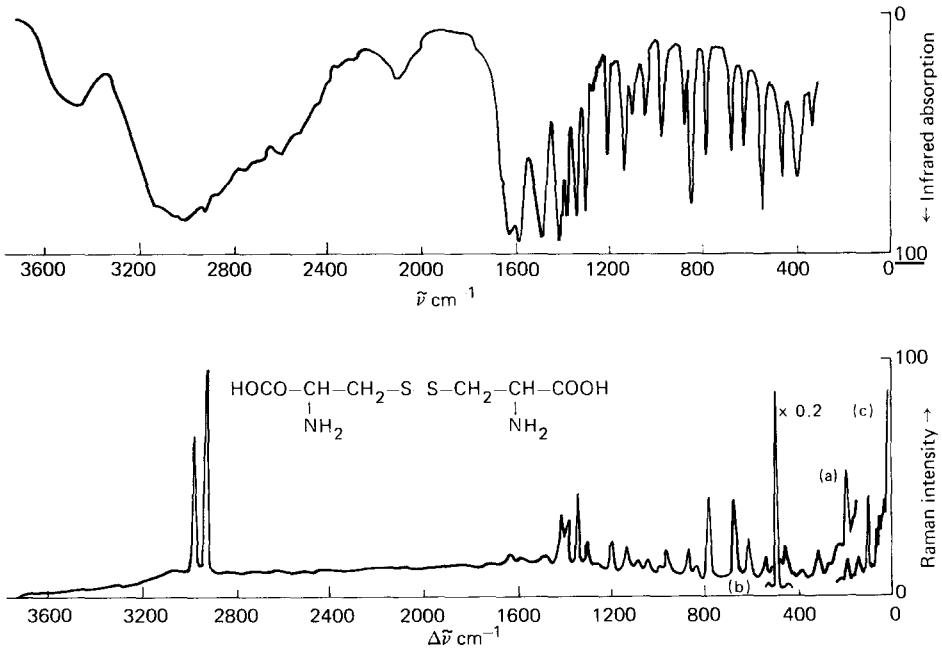

Fig. 25. Infrared and Raman spectra of crystalline cystine. Infrared spectrum of 0.8 mg in 400 mg KI; Raman spectrum (a), 2 mg, amplification ×1; (b), 2 mg, amplification ×0.2; and (c) disc, 140 mg, amplification ×0.3. (From ref. [2]).

This symmetry selectivity generally results in a simpler Raman spectrum than IR, a factor which is extremely useful in structure elucidation. A few examples will illustrate these points and emphasize the complementary nature of Raman and IR. Many more examples of this natural partnership for general vibrational analysis have been given by Washburn [63]. Fig. 25 shows the IR and Raman spectra of crystalline cystine. The NH_3^+ stretching vibration completely dominates the IR spectrum in the 3000 cm^{-1} region whereas the Raman shows two sharp bands associated with CH and CH_2 stretching. Both the IR and Raman show the NH_3^+ deformation and antisymmetric vibrations of the carboxylate group $-CO_2^-$ near 1600 cm^{-1}, but in the Raman they are much weaker. A strong band at 1410 cm^{-1} due to symmetric carboxylate stretch is present in both the IR and Raman. The strongest band of the Raman spectrum, however, occurs at 410 cm^{-1}, due to –S–S– stretch; this band is not nearly as apparent in the IR.

Fig. 26 shows the IR and Raman spectra of 2,5,5-dimethyl–3-phenylpyran-2(5H)-one. The greater simplicity of the Raman spectrum is quite evident. The C=C stretching vibration at 1640 cm^{-1} is very

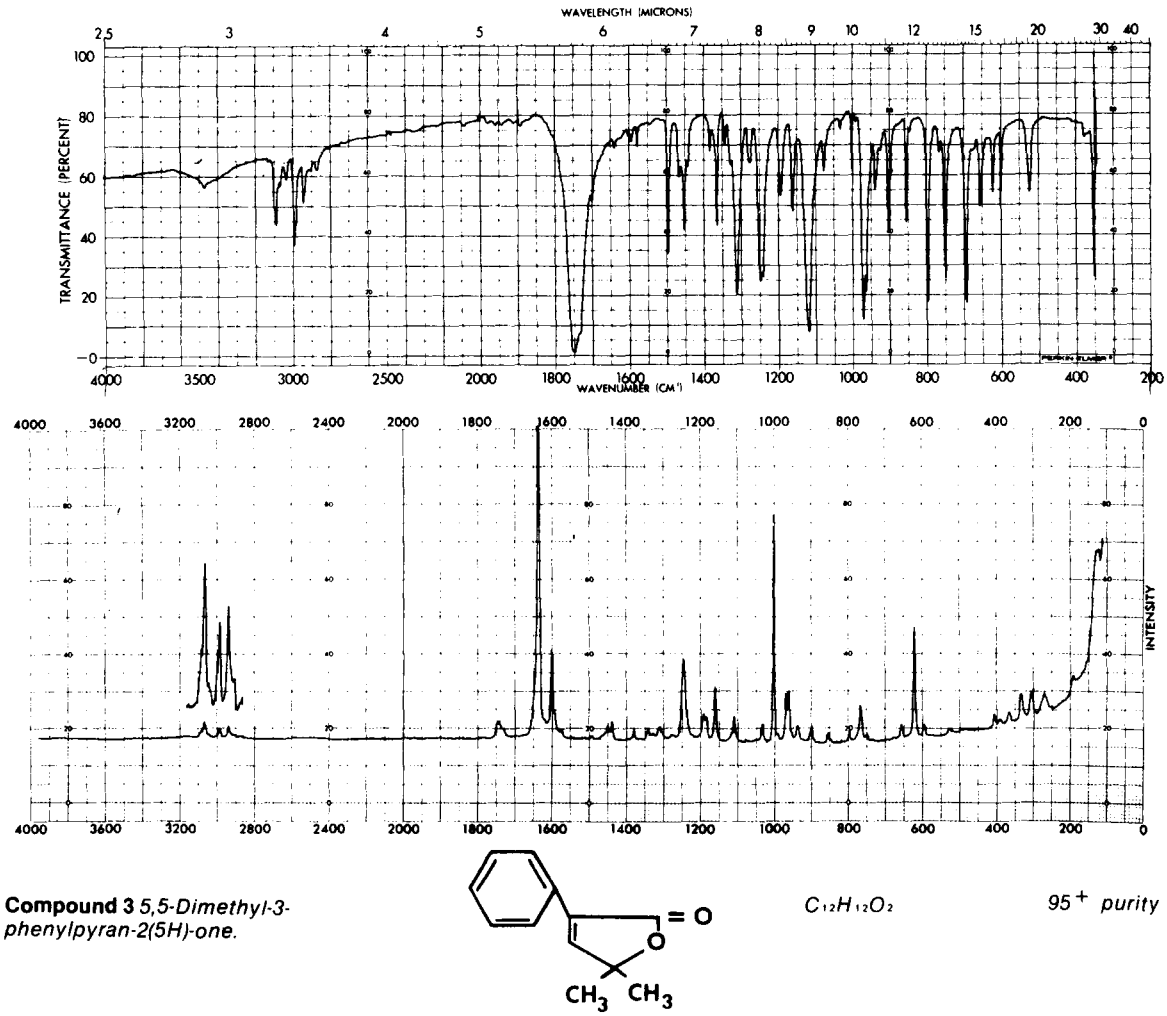

Fig. 26. IR and Raman spectra of 2,5,5-dimethyl-3-phenylpyran-2(5H)-one. (From ref. [63].)

strong in the Raman but barely visible in the IR. On the other hand, the C=O stretch at 1700 cm^{-1} is only observed in the IR. The IR bands at 750 and 700 cm^{-1} due to a monosubstituted benzene ring are present but difficult to identify in such a complex spectrum. The Raman more clearly defines the substitution pattern from the ring doublet near 1600 cm^{-1}, the ring in-plane bending near 618 cm^{-1}, and ring deformation at 1000 cm^{-1} with a shoulder at 995 cm^{-1}.

Another observation in the IR and Raman spectra is that the Raman bands show a greater variation of intensities, ranging from very weak to very strong. This seems to be a general characteristic evident when comparing IR and Raman spectra.

6.2. Studies of structurally related compounds

There have also been extensive studies of Raman vibrations for a number of specific types of compounds. Alkyl benzenes with 3 to 15 C atoms in the alkyl chain were investigated by Behroozi et al. [64]. The chloromethyl group attached to an aliphatic hydrocarbon chain was examined by Wang and Mannion [65]. Lere-Porte et al. studied the CH_2 vibration of ethane disubstituted by polar groups such as OH and halogens [66]. Nyquist [67] established the characteristic Raman bands for phthalate esters from a study of 21 compounds.

Freeman and Mayo [68] examined the thiomethyl group in various monosulfides, disulfides and trisulfides. The latter two authors also reported on the spectra of 70 di- and trisubstituted acyclic and cyclic compounds containing methyl groups situated on ethylenic carbon atoms [69]. A good correlation was obtained between the number of methyls directly attached to ethylenic carbon atoms and the intensity ratio of the methyl symmetric deformation mode (ca. 1375 cm^{-1}) to a band at 1440 cm^{-1}.

Saturated long chain fatty acids have been studied by Warren and Hooper [70] for a relationship between wavenumber shifts of the longitudinal acoustic vibrations of the carbon skeleton called accordion modes and the chain length (C_{12}–C_{24}) of the acids.

There have been a number of studies of benzene derivatives which provide information both on the nature of the substitution pattern and the interactions of the substituents [50, 71]. In these cases, however, one band alone is of little value – – the existence, position, and intensity of a number of bands have to be considered. This type of information can be classified into simple yes and no answers which provide a scheme for the determination of the substitution type [43] as shown in fig. 27. Such flow diagrams have also been devised by Willis et al. for barbiturates [72] and by Oertel and Myhre for substituted pyrazines [49]. Visser and Van der Maas have published a series of 4 papers describing systematic procedures for the interpretation of Raman spectra of carbon-hydrogen and alcoholic compounds [73], ethers (based on 80 compounds) [74], carbonyl-containing compounds (based on 220 ketones, aldehydes, esters and acids) [75], and nitrogen-containing organic compounds (based on 79 amines, pyridines, cyanides, amides, and nitro compounds) [76]. A total of 606 compounds, including all groups, were examined. The system contains 376 question or Q elements and 178 information or I elements and is now available on a Fortran IV program. The authors hope to extend the system with other functionalities but plan to set up rules and procedures first to overcome interferences caused by the larger growing number of functionalities and related frequency intervals.

A similar systematic empirical evaluation of frequencies and intensities has been developed for Raman steroid spectra [77–79]. It enables predictions about the number and intensities of multiple bonds and about the cis and trans coupling of rings A and B by using the CH_2 and CH_3 vibrations near 1450 cm^{-1} as reference groups. If there are the strongest bands in the spectrum, a saturated structure is indicated. If there are only bands stronger than the reference group above 1450 cm^{-1}, isolated or

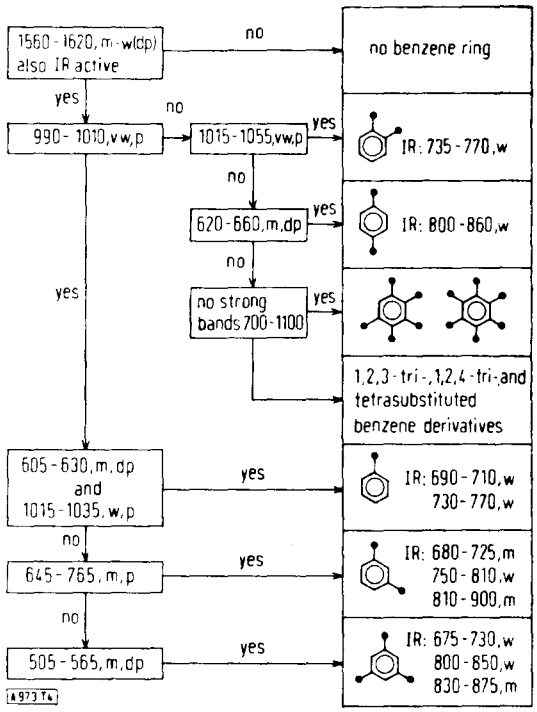

Fig. 27. Scheme for the determination of the substitution pattern of benzene derivatives with the aid of characteristic bands in the Raman spectrum; intensities: m medium, s strong, vs very strong; degree of polarization: p polarized, dp depolarized. IR denotes characteristic band in the IR spectrum. (From ref. [43].)

conjugated double bonds at the five-membered ring D or homoannular dienes are likely. The presence of conjugated double bonds in or at the 6-membered rings leads to stronger bands both above and below 1450 cm^{-1}. Information concerning the nature and position of these structural elements can be obtained from the number and frequencies of these bands [43].

All of these logical analytical schemes can readily be adapted to a computer and, together with IR, UV, NMR, or mass spectral data, can be used for identification of unknown compounds.

6.3. Conformation studies and molecular symmetry

Raman spectral data utilizing molecular symmetry and normal vibration frequencies of representative organic molecules can be an aid to conformation studies and subsequent predictions of the expected spectra of larger and more complex molecules. The group theory method for calculating the number of vibration modes in each symmetry class and the number of corresponding lines in the spectrum has been explained by a number of authors including Sushchinskii [80]. Comparison of the calculated results with experimental data allows improvement of the molecular constants used in calculations and development of a detailed interpretation of the observed spectrum.

Many papers have been published involving conformational studies; only a few examples will be listed here. Buge, Reich and Steger [81] studied the IR and Raman spectra of liquid and solid diethylmaleate and fumarate. They confirmed a previously reported conformational equilibrium for the diethyl fumarate and found at least two conformers in liquid dialkylmaleates.

Manley and Martin [82] recorded the IR and Raman polarized spectra of methyl, n-butyl (BMA) and n-octyl (OMA) methacrylates. They proposed complete assignments on the basis of C_S symmetry. They also discussed assignment of the torsional skeletal modes and interpretation of additional bands in the spectra of BMA and OMA.

Maillois et al. [83] investigated the Raman spectra of aqueous and D_2O solutions of fumaric and maleic acids. When combined with IR data, the results indicated that the fumaric acid was planar (C_{2h} symmetry) and that the maleic acid was non-planar, belonging to either the C_S or C_2 group.

Lewis and Laane [84] have recorded the vibrational spectra of 3-cyclopentene-1-one in the vapor, liquid and solid phases and carried out a complete vibrational analysis of the molecule. The spectra are in agreement with the planar C_{2V} structure.

Many more examples of conformational studies are given in the recent Annual Reviews of Raman literature published by Analytical Chemistry [85–87].

6.4. *Molecular potential functions*

Another area where Raman spectroscopy can be applied is the study of intramolecular forces, the knowledge of which is essential to a complete understanding of the properties and behavior of organic compounds. Molecular potential functions, which are related to energy barriers of various conformational states, can be obtained from the overtones of ring-puckering and internal torsional modes and thus, the conformation of the lowest energy state can be determined. Studies have been made on molecules such as 1,3-butadiene [88], styrene [89], glyoxal [90], acrolein [91] and a series of substituted ethanes [92–94]. Potential constants (cm^{-1}) and the most stable forms for the molecules studied are tabulated in table 8. Ring puckering vibrations have been identified and inversion barriers calculated also from the spectra of various small ring compounds [95–97].

6.5. *Physical properties*

Raman can also be used to study various types of physical properties – – hydrogen bond strengths, acid dissociation constants, phase transitions, and energy differences between rotational isomers.

Perchard and Perchard [98] studied several OH (OD) stretching vibrations of alcohols for frequency shifts as a function of temperature and intensity and polarization changes as functions of temperature

Table 8
Potential constants and most stable forms

	V_1	V_2	V_3	V_4	V_6 (cm^{-1})	Most stable form
1,3-butadiene	600	2068	278	−49		trans
glyoxal	1182 ± 10	1114 ± 10	–0–	−56 ± 4	–0–	trans
acrolein	306	1919	338	−96	−57	trans
styrene	–0–	623 ± 8	–0–	27 ± 3	–0–	planar
	V_1	V_2	V_3		V_6	
$CH_3CH_2NH_2$	218 ± 52	–0–	251 ± 17		−52 ± 11	trans
$CH_3CH_2PH_2$	–0–	270 ± 27	830 ± 17		−58 ± 10	trans
CH_3CH_2SH		171 ± 2	484 ± 1		−21 ± 1	gauche
CH_3CH_2SeH		−96 ± 1	432 ± 1		−20 ± 2	gauche

and physical state. Alcohols were also examined for hydrogen bonding effects by Lavrik and Naberul-chin [99], and hydrogen bonding in aqueous acid solutions was discussed by Pernall et al. [100].

Halogenated cyclohexanes have been studied in the vapor phase, in melts, in solutions and in amorphous solids for conformational information [94–95]. This work was later extended to include cyano- and isocyanatocyclohexane [101–102].

The energy differences between rotational isomers of 2-chloroethanol and 2-bromoethanol [103] and ethylene glycol [104] have been determined from their Raman spectra.

Variable temperature IR and Raman studies have enabled complete vibrational assignments to be made and thermodynamic functions for buta–1,3-diene and 2-methylbuta–1,3-diene (isoprene) to be calculated [105]. These thermodynamic functions, in turn, have permitted the equilibrium ratios between the s-trans and s-cis conformers at normal temperatures to be established.

The Analytical Chemistry Annual Reviews [85–87] give many more examples of the use of Raman Spectroscopy in studying changes in physical properties of organic molecules.

7. Raman applications to polymers

A large number of publications including some excellent review articles [106–109] discuss applications of Raman spectroscopy in studies of polymers. One of the real advantages of Raman spectroscopy in polymer characterization is the ease of obtaining a good spectrum with little or no sample handling. Injection-molded pieces, pipe and tubing, blown film, cast sheet or monofilaments can be examined directly. If the thermal history is important for understanding the properties of a plastic, it is clearly undesirable to melt or dissolve the sample, as may be necessary for IR spectroscopy. Also, different properties are associated with the amorphous as compared to the more ordered regions within a polymer, and the Raman spectrum, obtained on the sample in its state as a finished product from which the physical property information is obtained, is of great value. Filled polymers, like composites, contain fillers such as glass or clay which strongly interfere with the infrared spectra of the polymer because of their own intense absorption. On the other hand, glass and clay are poor Raman scatterers, so the Raman spectrum can be obtained without removal of the filler or any preparative techniques.

Raman is extremely valuable in many different areas of polymer characterization. In addition to the identification of the specific type of polymer, it can be used to determine functional groups, end-groups, structure, conformation, and orientation of chains, and to follow changes in structural parameters as the polymers are exposed to environmental or mechanical stresses [110]. Table 9 rates the usefulness of Raman for various kinds of polymer analysis.

Raman has also been applied to studies of the mechanisms of polymer reactions. Koenig [110] followed the polymerization of butadiene which can yield any of the different structures shown in fig. 28. The polymerization conditions determine the amounts of 1,2 and 1,4 structures formed, which are important because the relative concentrations of each present in the end product determines its properties. Unsaturation cannot be measured by the C=C stretching band in the IR because it is very weak (in fact, it is not observed for the 1,4 trans structure). However, the C=C is the strongest band in the Raman spectrum, and the type of unsaturation can easily be determined by its position.

The impact of data systems on the applications of Raman spectroscopy has already been described [6]. Fig. 29 shows the totally integrated system in the Sohio molecular spectroscopy laboratory where three dedicated minicomputers are utilized for instrument control, data acquisition, and data reduction of five instruments. RS-232 interfaces permit foreground, background operation and data output on any

Table 9
Uses of Raman spectroscopy

	Usefulness of Raman			
	Excellent	Very good	Good	Poor
Polymer				
Homonuclear backbone	×			
Polar substituents			×	
Endgroups				×
Multicomponent systems				
Additives (<1%)				×
Fillers (5%>)				
Glass	×			
Carbon black				×
Inorganic (TiO_2)		×		
Pigments			variable	
Properties				
Variable size and shape	×			
Limited solubility	×			
Colors with aging				×
Sensitive to thermal history	×			

instrument recorder. Grasselli et al. describe an example illustrating the versatility of the system to follow the extent of cross-linking in an experimental polystyrene polymer [41]. The sample was insoluble in typical NMR solvents and, because of the high sensitivity in the Raman for C=C absorptions, Raman was selected over infrared analysis as the analytical method. The powdered samples were packed into a capillary tube and the spectra were recorded over the region from 1700 to 1500 cm^{-1}. The Raman spectrum shown in fig. 30 was plotted on the Nicolet FT-IR spectrometer. Its presentation is in infrared format with peaks going down, rather than in Raman format with peaks going up. To follow the extent of cross-linking, the area of the C=C at 1645 cm^{-1} due to the cross-linking agent was ratioed to the area of a polystyrene ring absorption at 1590 cm^{-1} which was used as an internal standard band. The integration was performed using an NMR program on the Nicolet 1080

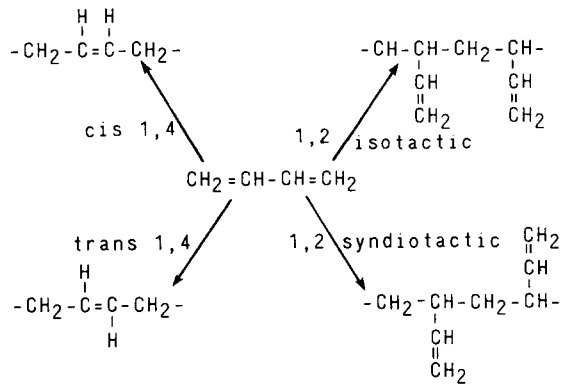

Fig. 28. Butadiene polymerization mechanisms. (From ref. [110].)

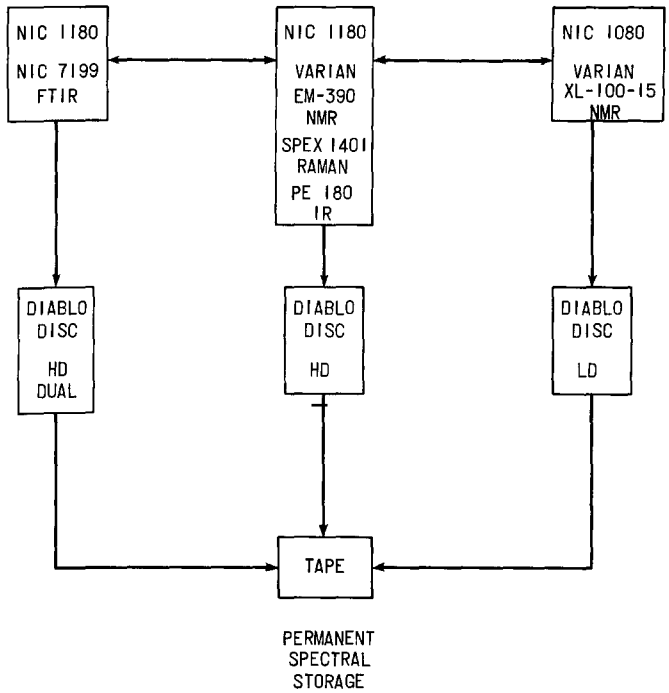

Fig. 29. Integrated data system in Sohio molecular spectroscopy laboratory. (From ref. [41].)

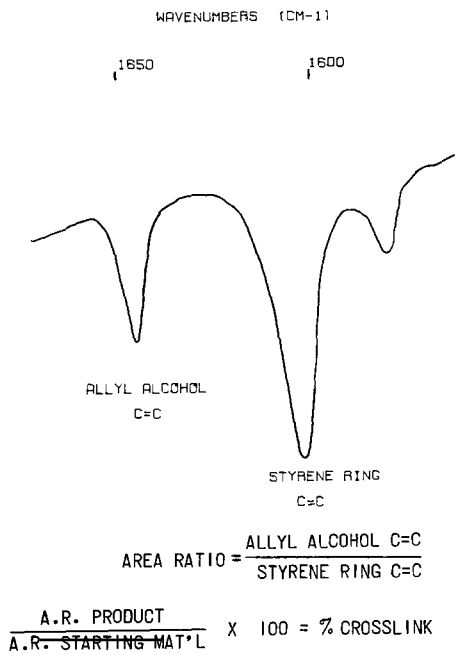

Fig. 30. Raman spectrum showing the extent of cross-linking in an experimental polystyrene polymer. (From ref. [41].)

computer. The ratio of the two band areas for the starting material was compared to that for the product. The extent of cross-linking was followed very rapidly by watching the disappearance of the C=C absorption due to the cross-linking agent, allyl alcohol, as compared to the C=C of the polystyrene.

In a similar example the extent of cure in a polyester resin was measured by Raman spectroscopy. Again, Raman was utilized because of its high sensitivity and specificity to C=C absorptions. The samples were polystyrene-based polyester resins and a method was established using the band at 1625 cm^{-1} due to the symmetrical stretching vibration of the vinyl C=C in the monomer, styrene, and the 1590 cm^{-1} band due to the aromatic ring structure [41].

Other polymer compositional analyses have been done with Raman. Meeks and Koenig have made quantitative measurements on copolymers of vinyl chloride and vinylidene chloride [111–112]. Boerio and Yuann reported compositional analysis of styrene glycidal methacrylate and methyl methacrylate-glycidal methacrylate copolymers [113]. Sloan and Bramston-Clark published quantitative results in a three component polymer system [114] containing styrene, butadiene and methylmethacrylate. Mukherjee et al. [115] developed a method for the determination of terminal thiol groups in sulfur polymers using ethyloxyacetate as an internal standard.

7.1. Polarization measurements of polymers

Raman polarization measurements on polymers can provide extremely valuable structural information, but they are sometimes difficult to obtain. Optical clarity and fluorescence can cause trouble, especially with impure or chemically complex samples. Another problem, specific to polarization studies, is the scrambling caused by multiple scattering in a heterogenous system [116]. Solutions to these problems include a combination of careful sample handling and sophisticated measuring techniques.

The basic equipment necessary for polarization measurements on polymers has been described by Shepherd [117], Hendra [109], and Gilson and Hendra [118]. More sophisticated equipment is necessary if any of the problems outlined above are serious, and this has been described by Shepherd [116].

Molecular conformation studies are extremely dependent upon accurate polarization measurements. Disordered polymers give vibrational modes which are all active in the infrared and Raman, and all of the Raman lines are polarized. Polyvinyl fluoride is an example [112]. Ordered structures show substantial differences in IR and Raman frequencies, therefore making it necessary to include Raman polarization and infrared dichroic measurements to determine the conformation of the chain.

Jasse and coworkers [119] recently described the influence of the chain conformation on the ν_1 and ν_{13} normal modes of the benzene ring in atactic and isotactic polystyrene. A series of model compounds whose conformations were confirmed by NMR analysis were used to establish the band assignments. It was found that the ν_1 mode is influenced by the local conformation of the alkyl chain as well as by the length of the conformation structure along the chain. The ν_{13} mode is only influenced by the local conformation and is insensitive to the length of the alkyl chain.

Changes in conformation as polymers are put into aqueous solution can also be followed since water is not a strong Raman scatterer. Koenig et al. [120] studied the structure of polyethylene oxide (PEO) in aqueous solution. Fig. 31 shows the spectra of crystalline PEO and a 10% water solution PEO. The crystalline spectrum is complex, showing several sharp bands with characteristic helical splitting. The spectrum of the melt has broader bands at shifted frequencies and no band splitting is detected. This indicates the helical structure of the solid polymer is lost upon melting. On the other hand, the spectrum of PEO in water looks much more like the crystalline polymer indicating that considerable helical structure is left upon dissolution.

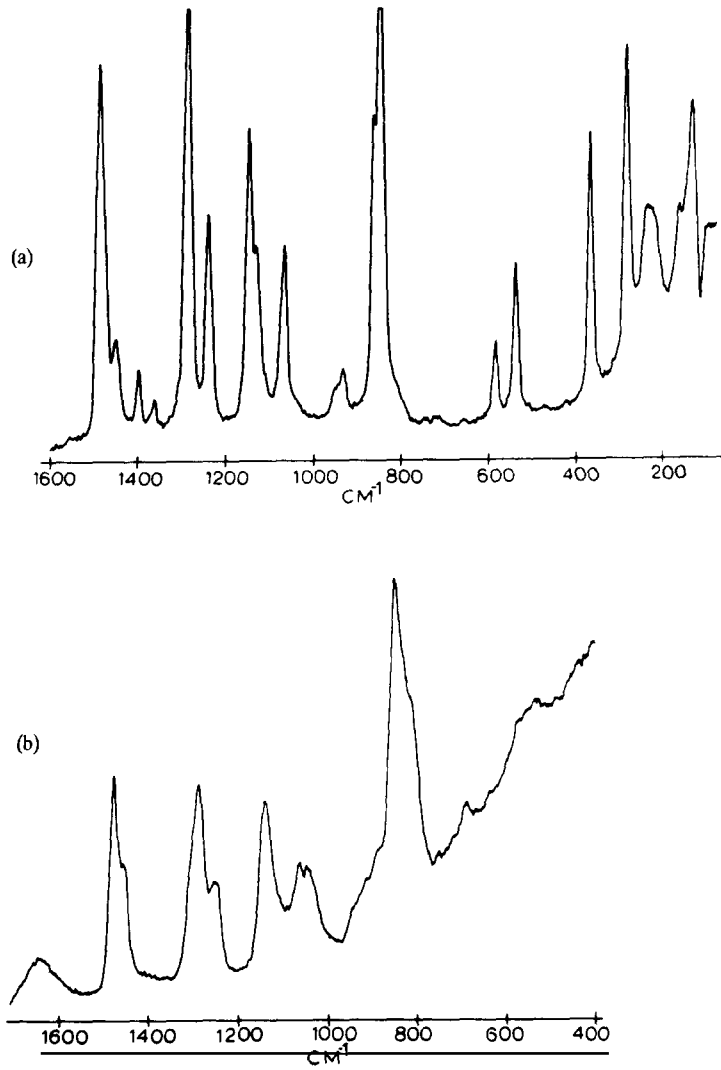

Fig. 31. Raman spectra of polyethylene oxide. (a), solid PEO; (b), 10% aqueous solution of PEO. (From ref. [120].)

Koenig [112] has summarized selection rules for Raman and infrared activity for monosubstituted vinyl polymers (fig. 32). These polymers can exist in a number of configurations. They may be syndiotactic or isotactic in a helical or planar conformation. Alternatively, they can be atactic with a disordered conformation. Each of these structures has its own selection rules. With the aid of such a spectroscopic scheme, ideally, it should be possible to unequivocally determine the structure of any unknown monosubstituted vinyl polymer.

Bailey et al. have used polarization data to determine mode assignments for isotactic polypropylene (IPP) [121]. The uniaxially oriented polymer was studied in a variety of geometries and some of these data are shown in fig. 33. Significant degrees of polarization were observed in spite of the incomplete orientation and optical scrambling. IPP, which has a 3_1 helical form (a helix with 3 monomers per turn), can be treated as belonging to a group isomorphous with the point group C_3; 25 normal vibrations can be classified as A modes and 52 as B modes. Both these species can be distinguished in the spectra, and the assignments agree well with previous IR [122] and Raman results [123].

STRUCTURE		SYMMETRY	OPTICAL ACTIVITY								EXAMPLE
			R	p	p	d	d	p	d	O	O
			IR	π	σ	π	σ	O	O	π	σ	
CENTER OF SYMMETRY		D_{2h} C_{2h}						√	√	√	√	PE, PES
ATACTIC			√	√	√	√					PVF
SYNDIOTACTIC	HELIX $>3_1$	D_n				√		√	√		PEO
	HELIX 3_1	D_3				√		√		√	
	HELIX 2_1	D_2			√	√		√			
	PLANAR	C_{2v}		√	√	√			√		PVC
ISOTACTIC	HELIX $>3_1$	C_n	√			√			√		POLYBUTENE
	HELIX 3_1	C_3	√			√					PP
	PLANAR	C_S		√	√						

Fig. 32. Selection rules for monosubstituted polyvinyl polymers. (From ref. [112].)

The Raman spectrum of the 2-fold helix of syndiotactic polypropylene has also been obtained and interpreted [124]. Chalmers found good agreement between observed and predicted shifts which verified the force field and proposed structure of Schachtschneider and Snyder.

Another important area of research in polymer studies involves how the physical and mechanical properties of a polymer are influenced by molecular orientation induced by drawing. Raman polarization studies can give detailed information about the distribution of orientations of structural units for both crystalline and non-crystalline regions. This has been evidenced in work on oriented poly(methylmethacrylate) (PMMA) [125–126] and poly(ethylene terepthalate) (PET) [125, 127]. Hendra and Willis [128–129] have studied oriented polypropylene and polyethylene; Derouault et al. have studied inhomogeous PET [130] and Gall et al. [131] have worked with polyethylene (PE), but none of these latter efforts included quantitative estimates of orientation.

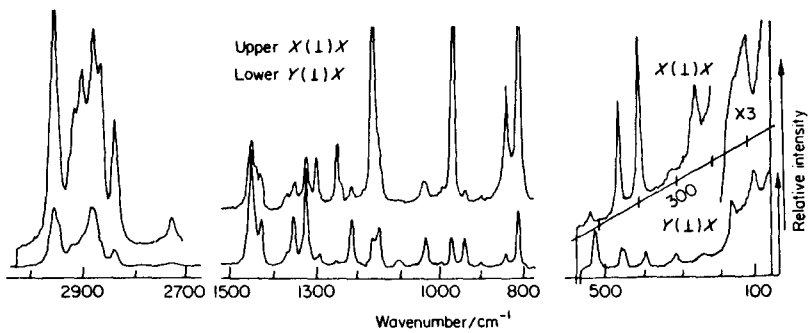

Fig. 33. Raman spectra of oriented isotactic polypropylene. The orientation axis is perpendicular to both the observation axis Y and the laser beam direction Z. In each spectrum the scattered polarization is X; the incident polarization is X (upper) or Y (lower). (From ref. [121].)

Table 10
Orientation functions for oriented polyethylene films[a]

Band	Assignment	From Raman data		From IR data	Theoretical	
$\tilde{\nu}/cm^{-1}$		$\cos^2\theta$	$\cos^4\theta$	$\cos^2\theta$	$\cos^2\theta$	$\cos^4\theta$
1081	Amorphous (gauche isomer)	0.415	0.334	0.45	0.45[b]	0.31[b]
1170	a_g+b_{1g}	0.831	0.763	0.85	0.83[c]	0.74[c]

[a]J. Maxfield, R.S. Stein and M.C. Chen, J. Polym. Sci., Polym. Phys. Ed. 16 (1978) 37.
[b]Based on ref. [132].
[c]Based on ref. [133].

Quantitative calculations of molecular orientation have been made for polyethylene and these have been summarized by Shepherd [116] in table 10. The studies used two PE "crystalline" bands at 1170 cm^{-1} and 1296 cm^{-1} and one "amorphous" band at 1081 cm^{-1}. Values of the averages $\cos^2\theta$ and $\cos^4\theta$ were calculated, where θ is the angle between a unique axis in the unit and the draw direction. IR results for $\cos^2\theta$ are also included in the table and the agreement with the Raman measurements is good. Theoretical calculations were also made using a rubber elasticity model for the amorphous band [132] and a spherulitic model [133] for the crystalline averages. Again, the agreement is surprisingly good.

Quantitative data was also obtained on chain orientation in hydrostatically extruded polypropylene by Satija and Wang [134]. The alignment of the polymer chain along the direction of extrusion was found to increase with the increase of the extrusion ratio.

7.2. Morphological effects

Morphological effects in polymers can readily be studied by Raman. Many polymers solidify from the melt in spherulites composed of lamellar structural units. Measurement of the detailed structure of lamellae is of great interest to polymer chemists because of its relationship to mechanical strength and stability of the material [135–136]. Although X-ray diffraction, electron microscopy, and differential scanning calorimetry are commonly used to obtain information on crystallinity and lamellar thickness, Raman has also been proposed as a convenient and rapid technique for measuring the dimensions of chain-folded lamella. A low frequency Raman band in n-paraffins has a frequency that is inversely proportional to chain length. The band was assigned to the fundamental longitudinal acoustic mode (LAM) of the chain and was observed in polyethylene, poly(ethylene oxides) and polypropylene [137]. The LAM was used by some workers to measure "chain length" and lamellar thickness, but an elegant theoretical treatment of the LAM has been published by Krimm et al. [137] which shows that the LAM frequencies are affected by perturbing forces in the ends of the chains as well as by relative moduli, densities and fractions of amorphous and crystalline components. Nevertheless, Raman spectroscopy is extremely helpful in determining the mechanism of lamellar formulation, the structure of fold sequences, and the nature of interlamellar adhesive forces. Deformation and cooling effects on the lamellar structure of high density polyethylene have already been studied [138].

7.3. Other polymer features

In addition to conformation and configuration, Raman spectra are sensitive to other polymer features

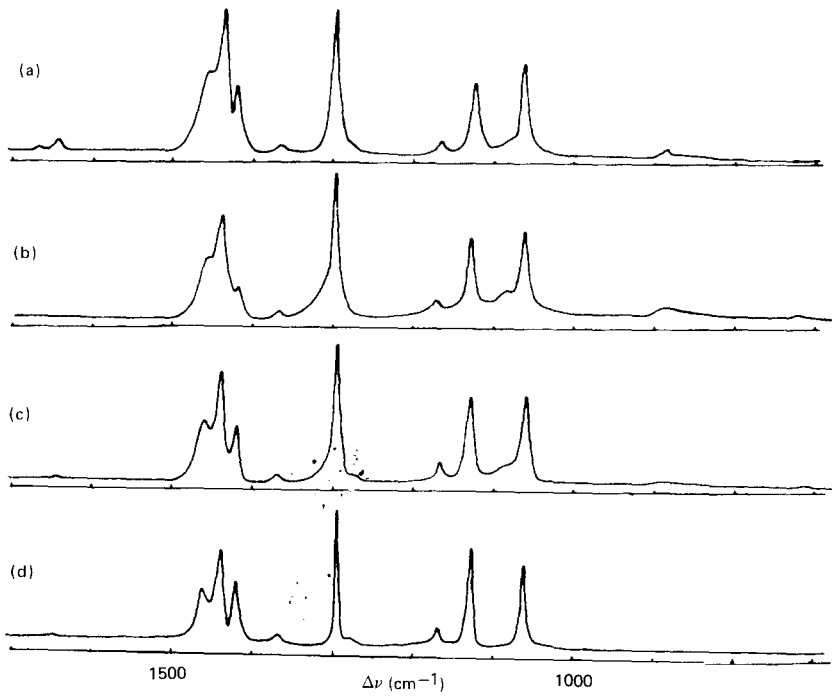

Fig. 34. Raman spectra of some polyethylenes. In (a) the Raman spectrum of a wax lump with molecular weight around 800 is shown. It melts around 75°C. An unoriented film gave the spectrum in (b). Spectra of high density, high melting point forms with a molecular weight 10^4–10^5 are shown in (c) and (d). The intensity of the feature at 890 cm^{-1} is a rough inverse indicator of the molecular weight. Crystallinity, a desirable characteristic from the standpoint of oxidative degradation, is indicated by the sharpness of the bands at 1300 cm^{-1} and 1400–1500 cm^{-1}. Thus (b) with a crystallinity of 50% exhibits the widest Raman lines; (d) with almost total crystallinity (the extended chain form) shows the narrowest lines. When molecular chains terminate in a vinyl grouping, the features around 1650 cm^{-1} appear. (From ref. [139].)

such as the degree of crystallinity, chain folding, molecular weight and end groups [139]. Some of the special changes associated with these factors can be seen in fig. 34 which shows the Raman spectra of various forms of polyethylene. Consideration of molecular weight, degree of crystallinity, etc. is important because of the relationship of these factors to physical properties such as hardness, brittleness, permeability, impact resistance, etc. The end use dictates the structure and type of polyethylene needed.

7.4. Detection of impurities in polymer films

Raman is also a very effective technique for examining impurities in polymer films [136]. If caution is taken to prevent thermal decomposition of the sample, the laser beam can be condensed with a lens to examine specks of material with dimensions on the order of 100 μm. As opposed to IR, there is no problem with the direct beam entering the monochromator since the scattered light is collected at either 90° or 180° to the axis of the exciting beam. Also, there is no distortion of the Raman spectrum if the sample is irregular in shape or thickness.

Fig. 35 shows the spectrum of an ethylene vinyl acetate film containing a small speck of foreign material suspected to be another polymer. Also included in the figure is a reference of "pure" ethylene vinyl acetate and two suspected impurities – – low and high density polyethylene. Although the spectra are generally very similar, small differences can be noted. For example, the high density PE has a band

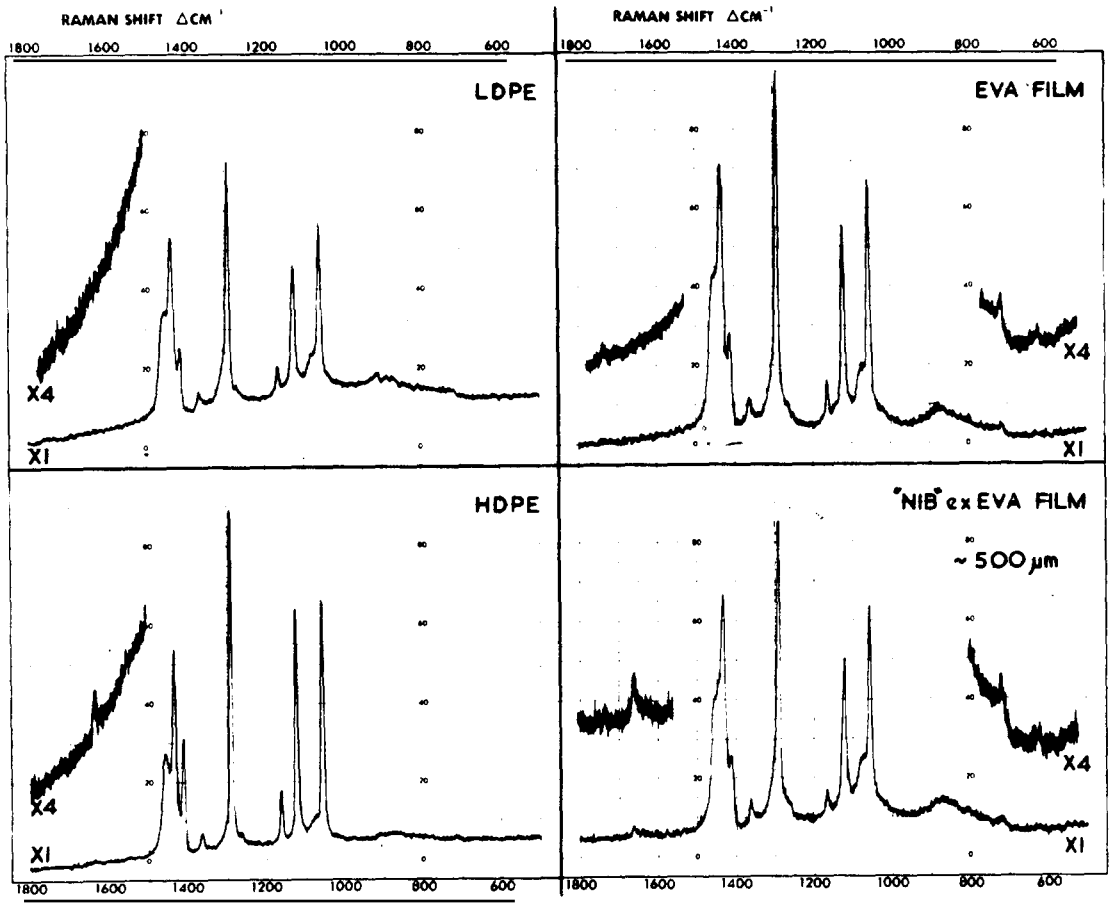

Fig. 35. Raman spectrum of impurity from a polymer film, and spectra of associated materials. (From ref. [136].)

at 1640 cm^{-1} assigned to terminal vinyl $-C{=}CH_2$ groups which does not appear in the low density PE. The spectrum of the impurity also shows unsaturation, but it occurs at 1660 cm^{-1} and is assigned to trans –CH=CH. This type of unsaturation occurs when ethylene-vinyl acetate copolymer is heated and acetic acid evolves. Thus, the impurity appears to be due to thermal decomposition of the polymer and not to either type of PE.

7.5. Miscellaneous polymer applications

There have been many Raman applications to studies of specific polymers or types of polymers. In the area of rubber chemistry, Coleman et al. measured Raman spectra of vulcanizates prepared from cis-1,4 polybutadiene, 2-mercaptobenzothiazole, sulphur, zinc oxide and lauric acid [140]. A technical review gives Raman evidence supporting a mixed free radical and ionic mechanism for accelerated sulfur vulcanization [141]. In a separate publication, Coleman et al. also assigned Raman bands to the crystalline and amorphous components of chloroprene polymers [142]. Crystallinity was studied in ethylene-propylene rubbers by Schreier et al. [143].

Several acrylic polymers have been examined using Raman. In addition to the orientation studies on poly(methyl methacrylate) already mentioned [125–126], the low frequency spectrum has been obtained

and discussed [144]. The neutralization of syndiotactic polyacrylic acid in aqueous solution was examined by Bardet et al., and a planar zig-zag configuration was observed for the non-ionized acid and its Na salt [145].

Maddams and coworkers [146–147] have used Raman spectroscopy in structural studies on polyvinylchloride. They obtained more complete assignments of the carbon–chlorine stretching modes through detailed analysis of band positions and band shapes, using computer resolution of overlapping bands to refine the information content. Of equal interest, analytically, was their characterization of polyene sequences between 9 and 17 conjugated double bonds in degraded polyvinylchloride samples. Koenig extended this work using the 363.9 nm laser line to detect apparent sequences of 7 to 8 conjugated double bonds in polyvinylchloride [148]. Certainly the characterization of such sequences in degraded polymers suggests new possibilities, both in detecting the initiation of degradation from the appearance of short conjugated sequences and in measuring the longer sequences for which UV-visible spectroscopy fails. It is possible, too, that as the tacticity of the polymer changes, the degradation mechanism will be affected. Studies of this nature are underway [149].

The effect of cross-linking on the Raman spectra of epoxy resins has been studied by Lu et al. [150] and on unsaturated polyester resins containing styrene by Koenig et al. [151]. In the hopes of obtaining some insight into the fracture mechanism of polymers, the effect of mechanical stress on the Raman spectra of polypropylene, polycarbonate, polystyrene and nylon 6,6 has been examined [152].

The structural changes which occur in wool after annealing have also been investigated [153] by Shishoo et al. Results show that the CH_2 groups in wool have parallel polarization in the Raman which increases significantly after annealing. The authors have formulated the hypothesis that a large number of electrovalent intrahelix cross-linkages exist between the suitable side groups on the main polypeptide chain in the helix of annealed wool.

7.6. Future of Raman polymer studies

The future of Raman polymer studies appears to hold great potential for many different applications. Improved force fields should contribute to a better understanding of regular and irregular conformations of polymers [154]. Polymer crystal studies should add to the existing knowledge of intramolecular forces in crystals and their effect on stable polymer structures. Intensity studies should also be valuable. Perhaps most important, however, will be the increased use of vibrational spectroscopy to understand the relationship between structure and function, an understanding which could have an important impact on designing polymers for specific physical properties.

8. Raman applications to biological systems

An essential problem of modern biophysics is obtaining detailed structural information in solution or in phases of intermediate fluidity, such as membranes. In such problems Raman spectroscopy is emerging as an important tool, particularly when used in combination with other techniques. Table 11 summarizes some of the positive aspects of the application of Raman spectroscopy to biological samples. Only limited use has been made to date of isotopic substitution, but this will become more common for elucidation of assignments. Small sample sizes are a very important advantage of Raman over other solution techniques.

Table 11 also gives the negative aspects of applying the Raman effect to these problems. Many of

Table 11
Application of Raman effect to biological problems

Positive aspects	Negative aspects
1. Spectra may be obtained in all phases	1. Raman effect is weak
2. Aqueous solutions may be used	2. Fluorescence is $\sim \times 10^6$ as strong
3. Sensitive to conformational change	3. Only moderate structural resolution
4. Isotopic substitution affects spectra	4. Conclusions often rely on indirect methods
5. Small sample size (5 nl volume)	5. Photochemistry may interfere

these are general to all applications of Raman spectroscopy. Of these, fluorescence has thus far been the major problem, but the indirect nature of the conclusions obtained from Raman work may prove to be the ultimate limitation on its applicability.

8.1. Peptides and proteins

Vibrational spectroscopy has long been used for studying conformations of peptides and proteins. The so-called amide I and amide II bands were widely used in infrared spectra but were not readily observable in aqueous solution. In Raman spectra, primary use has been made of the amide I and amide III modes. The amide II band is generally very weak in the Raman spectrum. Fig. 36 shows an approximate description of these modes. The frequencies of these modes are sensitive to the angles Ψ

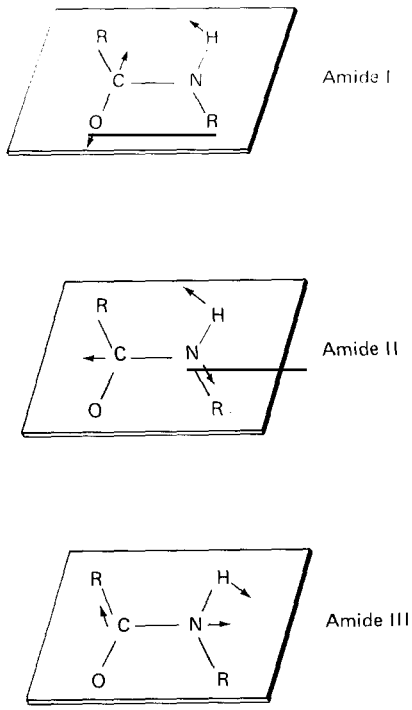

Fig. 36. There are many different modes of the peptide bond vibration. The figure illustrates the "in-plane" vibrational modes of the peptide bond. Among the three modes shown in the figure, the amide I and III are indices of peptide backbone conformation of a protein in the Raman spectra. The amide II band is either Raman inactive or very weak.

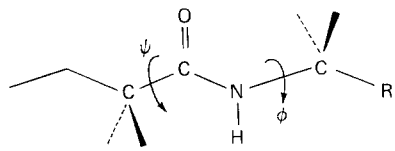

Fig. 37. Definition of the torsional angles ϕ and Ψ about the C^{α}–N bond and the C′–C^{α} bond. In the extended form shown, $\phi = \pm 180°$, $\Psi = 180°$.

and ϕ defined in fig. 37. Since these angles have characteristic values for the well known α helix and β sheet protein structures and a range of values for random coils, the modes are diagnostic for protein conformation in solution. Table 12 shows a summary of frequencies and intensities expected for various structures, and table 13 gives some specific examples of modes which have been observed for various peptides.

Poly-L-lysine spectra are a good example of the kind of information which can be obtained. Fig. 38 shows the spectra of α helical and β sheet forms of this peptide obtained by Peticolas [155]. These are in reasonably dilute aqueous solution. The amide I mode, concealed by a strong water band in the α helical form, appears strongly in the β sheet. Changes are also seen in the amide III region and the C–C stretching modes in the 945–1000 cm^{-1} region. One question related to these conformations which was answered by Raman spectroscopy was whether in transforming from $\alpha \rightarrow \beta$ the polymer goes through an intermediate structure, e.g. a random coil. This was not the case. A quantitative plot of the temperature dependence of the amide III intensity at 1240 cm^{-1} relative to another band in the spectrum allows the determination of the fraction of either conformer present.

In proteins, there is apt to be a distribution of conformers present in a single system. For such a case, the spectra are necessarily more complicated. Lord [156] has proposed that the intensity contour in the amide III region might be directly correlated with the distribution of Ψ values for the protein. An

Table 12
Conformation-sensitive Raman lines of peptidyl groups of aqueous proteins

σ (cm^{-1})	Assignment	Relative intensity	Conformational significance
1665–1672	amide I	strong	β-sheet
1660–1670	amide I	strong, broad	random chain
1645–1655	amide I	strong	α-helix
1270–1300	amide III	weak	α-helix
1243–1253	amide III	medium, broad	random chain
1229–1235	amide III	strong	β-sheet

Table 13
Amide III frequencies (in cm^{-1}) in polypeptides from Raman measurements

Substance	α-helical	β-structure	Random coil or structure ionized
Polyglycine	1261	1234	
Poly-L-alanine	1261	1239	
Poly-L-glutamic acid			1248
Glucagon	1266	1232	1248
Poly-L-lysine	1311	1240	1243
Poly Ala-Gly	1271	1238	
Poly Ser-Gly	1264	1236	

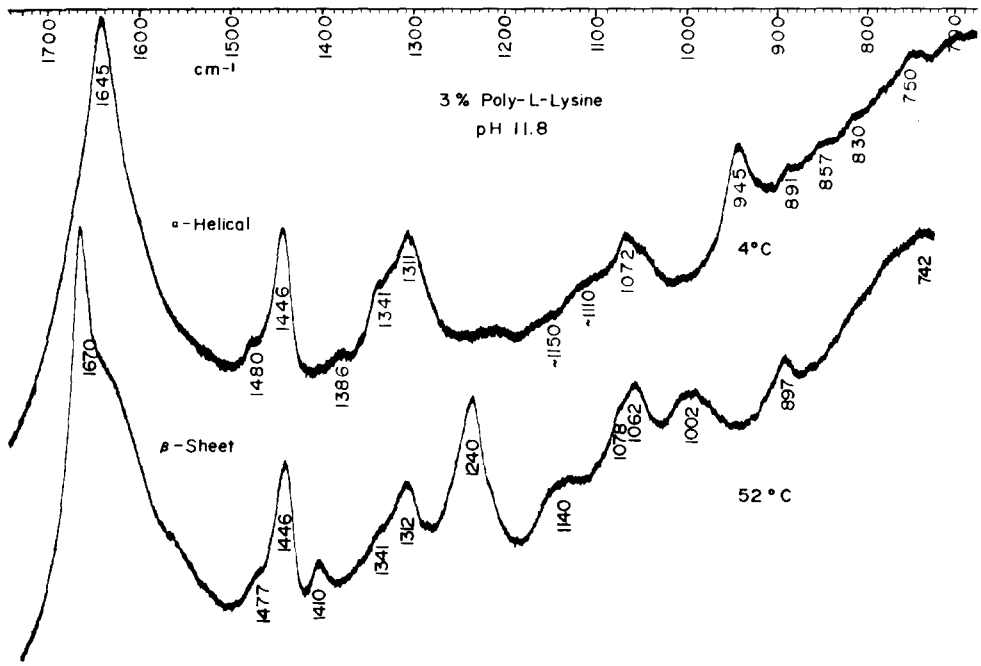

Fig. 38. Raman spectra. Upper, α-helical poly-L-lysine (3% H_2O, pH 11.8, $T = 4°C$) and lower, β-sheet poly-L-lysine (3% H_2O, pH 11.8, $T = 52°$). (From ref. [155].)

example of this approach, showing both the spectrum of a ribonuclease and a histogram representing the Ψ values for the enzyme is shown in fig. 39. More work is needed to establish the generality of the correlation.

A related approach to Lord's has been taken by Lippert et al. [157]. They suggest that four simultaneous equations can be used to establish quantitatively the fractions of α helix, β sheet, and random coil in a protein. To do this, they use the Raman intensities at 1240 cm^{-1} in H_2O solution and 1632 and 1660 cm^{-1} in D_2O, relative to the intensity of CH_2 deformation at 1448 cm^{-1}. Using poly-L-lysine as a standard to set the scale, they apply this method to nine proteins with good results (±10–15%). Craig and Gaber [158] have applied this method to a structurally well-documented enzyme, human carbonic anhydrase B, with good results as well.

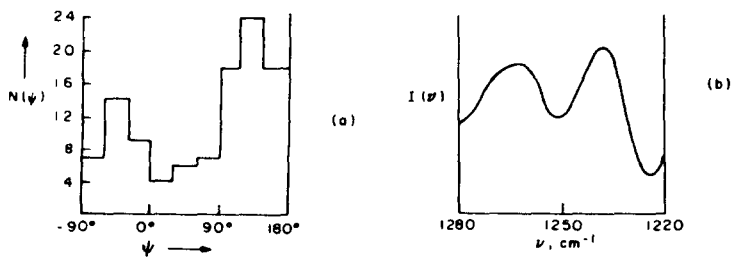

Fig. 39. (a) Histogram of distribution of values of Ψ in the range $-90°$ to $+180°$ in native bovine pancreatic ribonuclease and (b) Intensity contour of the amide III region in the Raman spectrum of the enzyme. (From ref. [156].)

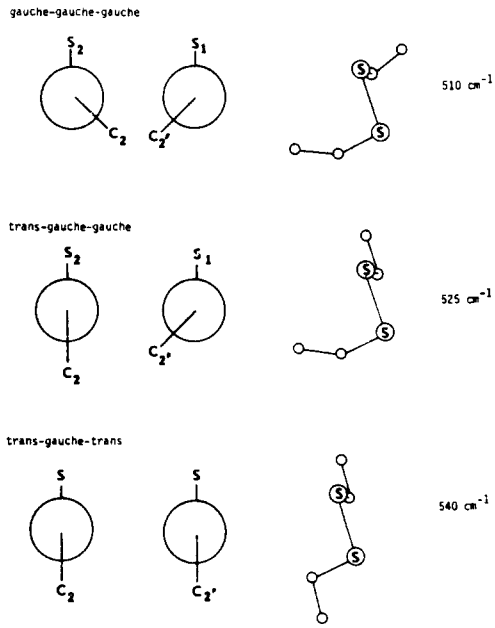

Fig. 40. Conformation of disulfide bonds in proteins. The stretching vibration of S–S is influenced by the rotational conformation about the C–C and C–S bonds. The assignment numbers for C and S atoms are: C_2–$C_1$$S_1$–$S_2$–$C_1$–$C_2$. The disulfide bond with gauche shows a strong and sharp band at 510 cm^{-1}. The disulfide bonds with trans–gauche–gauche and trans–gauche–trans conformation give bands at 525 and 540 cm^{-1} in Raman spectra. (From ref. [159].)

To maintain conformation of proteins, disulfide bonds are often built into the structure. The conformation about these disulfide bonds is often a crucial piece of information to be obtained in elucidating protein structure. Raman spectroscopy has proved to be useful for studying this problem. The polarizable sulfur atoms tend to give rather intense Raman scattering. Fig. 40 shows three possible cases and the S–S stretching frequencies observed for each. Fig. 41, a spectrum of a neurotoxin obtained from sea snake [159], illustrates an application of this by Yu and co-workers showing that the conformation is gauche–gauche–gauche. In a series of papers, Yu, Tu et al. [160–161] have shown that the snake neurotoxins are all primarily β sheet structures with gauche–gauche–gauche S–S linkages. Approximate molecular orbital methods indicate that there is a basis for the correlation of S–S frequencies with dihedral angle in the orbital overlaps obtained from a Mulliken population analysis [162].

8.2. Nucleotides and nucleic acids

While some work on peptides, amino acids, and proteins had been carried out using Raman spectroscopy prior to the laser era (that of Edsall and co-workers [163] is particularly notable), the spectra of nucleic acids and polynucleotides is more recent. A wide variety of problems have been studied by Raman spectroscopy with impressive results. Table 14, from Thomas [164], indicates the range of problems which have been investigated with some success. These include constitution, secondary structure, and dynamics. There have also been more sophisticated applications to protein-DNA or RNA interaction.

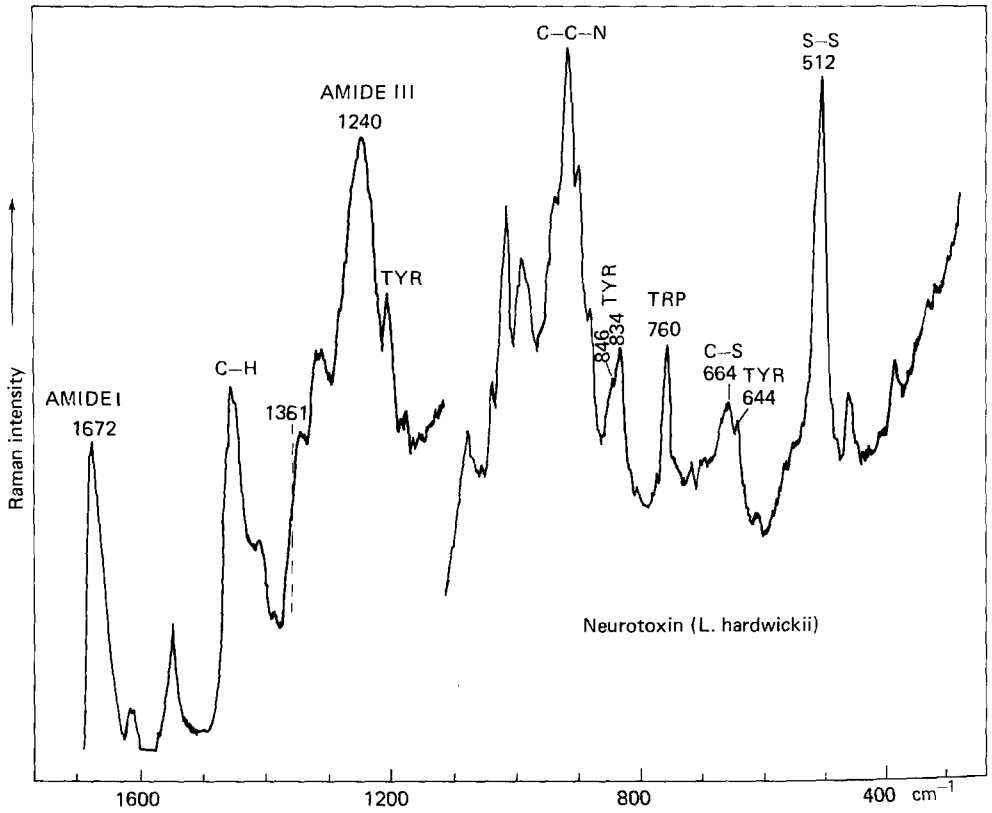

Fig. 41. Raman spectrum of purified sea snake neurotoxin. (From ref. [159].)

Table 14
Nucleic acid problems studied by Raman spectroscopy

1. Primary structures of nucleic acid constituents
   a. tautomeric equilibria of the purine and pyrimidine bases
   b. ionization equilibria of the bases
   c. ionization equilibria of the phosphate groups
   d. sites of deuterium–hydrogen exchange in base and sugar residues

2. Secondary structures and interactions of nucleic acids
   a. mode and extent of hydrogen bonding between bases
   b. mode and extent of base-stacking interactions
   c. identification of ordered and disordered backbone conformations
   d. order–disorder transitions as a function of temperature, ionic strength, etc....
   e. quantitative estimates of RNA secondary structure
   f. binding of metal ions to base and phosphate sites
   g. nucleic acid-protein interactions
   h. hydration of nucleic acids

3. Kinetics
   a. rate of exchange of 8-CH in purines
   b. rate of hydrolysis of nucleic acids

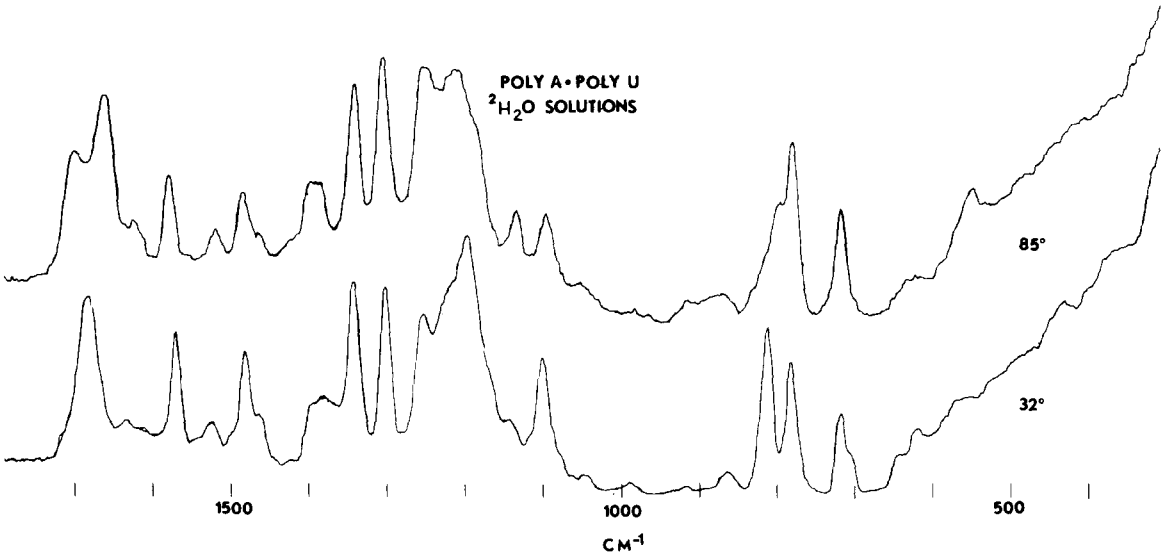

Fig. 42. Raman spectra of D_2O solutions of poly(A)·poly(U) at 32°C and 85°C. Solute concentration is 35 mg/ml. (From ref. [167].)

These studies illustrate well the importance of Raman spectroscopy as a technique for studying solution structures where the solid state structures have already been elucidated using crystallographic methods. There have been several extensive reviews of this work [165–166].

Thomas et al. [167] have carried out considerable work on the model systems poly(A), poly(U), poly(G) and poly(C), which can exist in double helical forms such as poly(A)·poly(U). Fig. 42 shows a spectrum of poly(A)·poly(U) in D_2O. There is a striking temperature dependence of this spectrum as the double helix dissociates to form two single stranded helices. This illustrates the sensitivity of Raman spectroscopy to such changes.

Fig. 43 shows spectra of tRNA taken in both H_2O and D_2O. Assignments of the various bands to nucleotide residues are indicated in the figure. Using an empirical assignment approach, it is possible to synthesize such spectra with some confidence from polynucleotide spectral fragments. The use of D_2O allows one to examine vibrations obscured by H_2O scattering, particularly in the 1650 cm^{-1} region. It also permits study of the exchangeable protons in the RNA. Chan and Thomas [168] have used this method to establish the kinetics of such exchange in one case.

In simple viruses, there exists a so-called coat protein which encapsulates RNA or DNA. The coat protein actually may consist of many protein molecules. Combining the work on protein spectra and nucleic acid spectra, the interactions between the nucleic acid and the protein have been studied by Raman spectroscopy.

Fig. 44 shows the spectra of two DNA virus particles, known as Pfl and fd virions [169]. High quality spectra are obtainable even from such complex systems. Because these particles are very high in protein content, this Raman scattering dominates the spectra. From the spectra one can learn a great deal about these systems. Drawing on correlations previously presented, one notes that both contain almost exclusively α helical protein; on the other hand, the amino acid compositions are seen to be quite different for the two cases. It is also possible to conclude that OH groups on the tyrosyl amino acid residues are strongly hydrogen bonded to positive donor groups in both cases. This is gleaned from the relative intensity of bands at 854 and 825 cm^{-1}. From model system work, it is possible to conclude that the DNA backbones are of the B helix type rather than the A helix. These brief summaries of

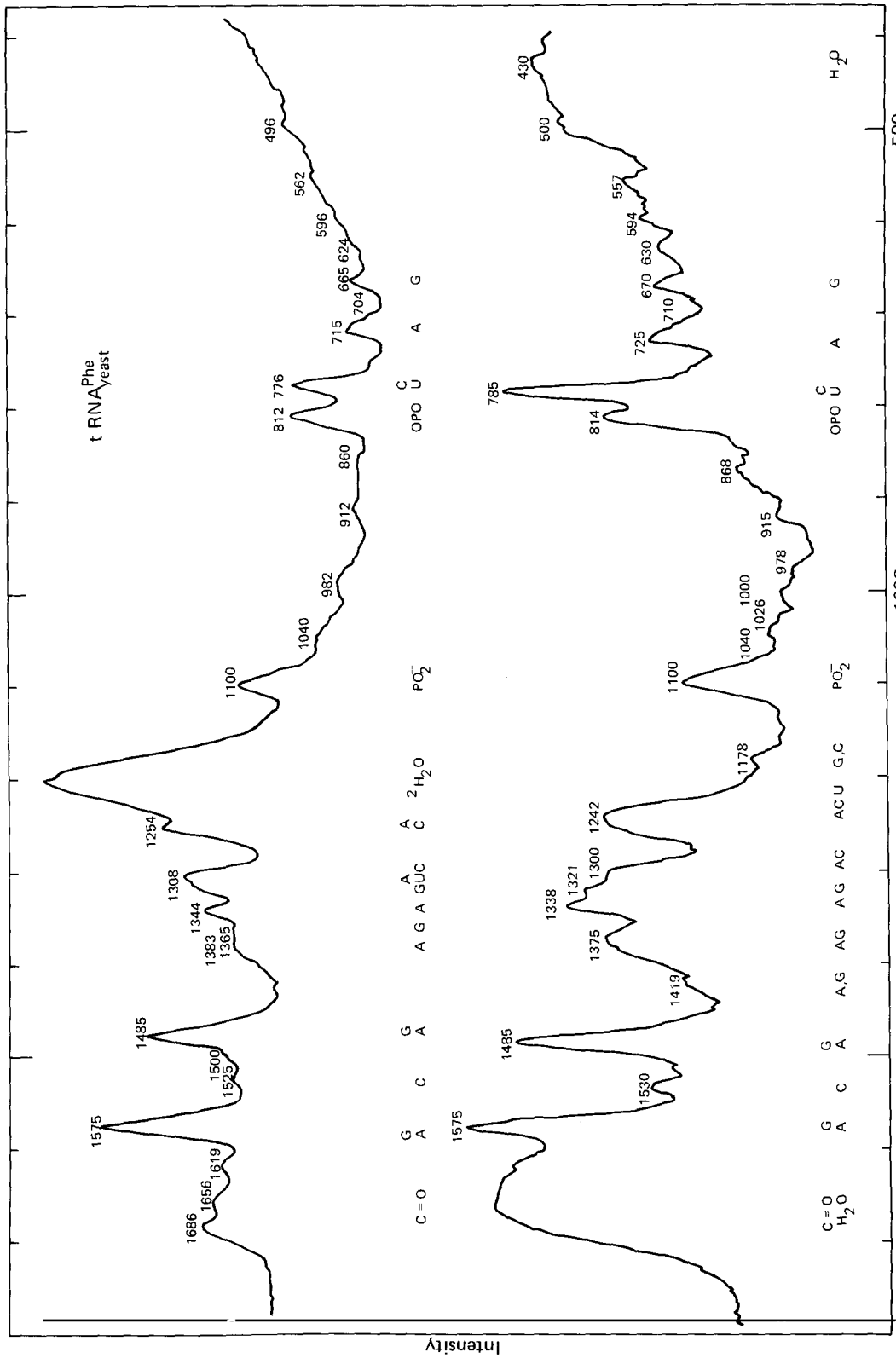

Fig. 43. Raman spectra of $tRNA^{Phe}_{yeast}$ obtained with 488.0 nm excitation. (a) H_2O solution, 40 μg/μl, *p*H7, 32°C; (b) D_2O solution, 40 μg/μl, *p*H7, 32°C. Frequencies of the prominent lines are listed in cm^{-1} units and assignments to base and backbone residues are indicated by letter symbols along the abscissa. (From ref. [168].)

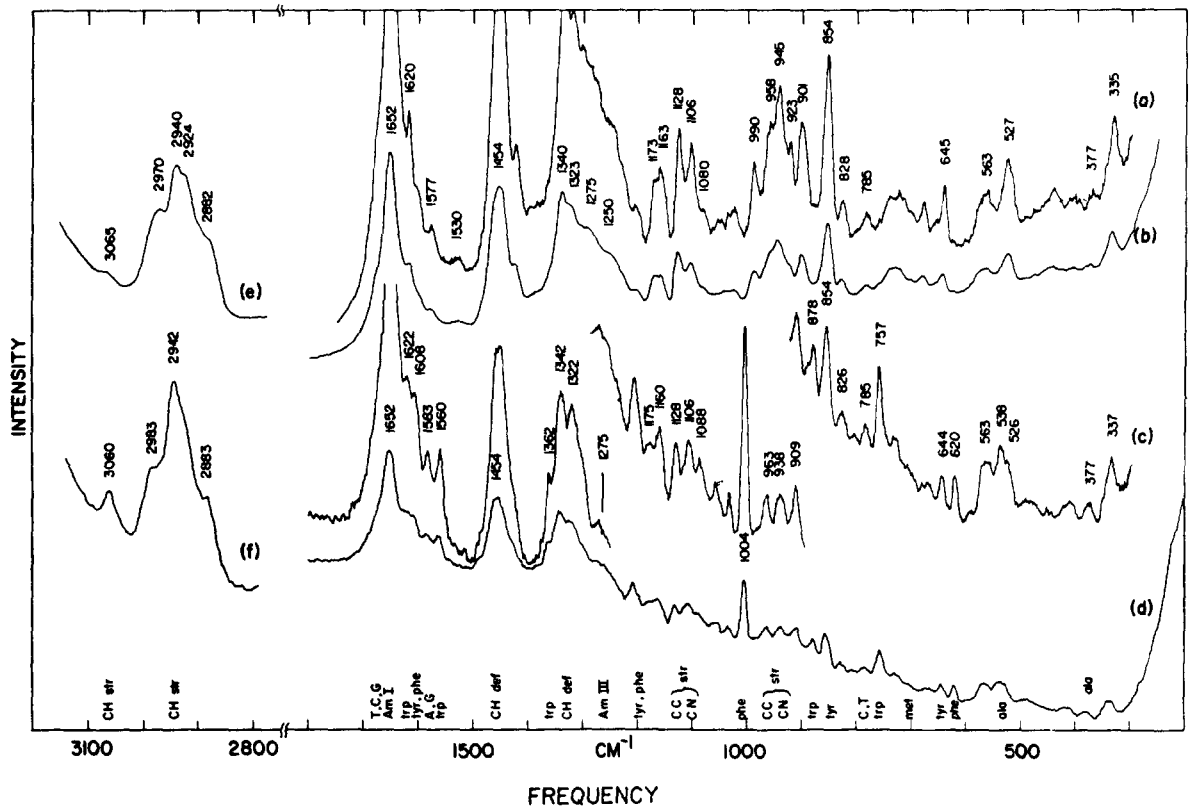

Fig. 44. Raman spectra of FB viruses in 0.05 M NaCl at 32°C and *p*H9. (From ref. [169].)

conclusions presented in great detail in the original work give an idea of the level of detailed information which can be extracted from the spectra.

8.3. Resonance Raman spectra of biological systems

Conventionally, Raman spectra require relatively high concentrations on the order of 0.1 M or greater. This may limit their application to real biological problems. However, when the Raman exciting line falls within the envelope of an electronic absorption band, it becomes possible to see Raman spectra at concentrations of approximately 10^{-5} M. Qualitatively, we may say that these spectra arise only from the part of the molecule associated with the electronic transition. Thus, in the case of a protein like hemoglobin containing a chromophore (heme) which is orbitally isolated from the bulk of the globin protein, we see a selectively enhanced spectrum.

Pioneering work on this problem was carried out by Spiro and Strekas [170]. They published the first spectra of resonance enhanced hemoglobin and cytochrome C. A particularly interesting feature was first observed in these spectra, although it had been predicted by Placzek, and other workers had attempted to observe it in model compounds without success. When the symmetry is either D_{4h} or slightly reduced from D_{4h}, certain modes have extremely large depolarization ratios. While in the non-resonance case the depolarization ratios range from 0 to 0.75, in this case values much greater than 0.75 are obtained. This results from the polarizability tensor being unsymmetrical to the point where α_{xy} may $= -\alpha_{yx}$.